Chapter 36

Neoproterozoic glacial record in the Mackenzie Mountains, northern Canadian Cordillera

P. F. HOFFMAN[1,2]* & G. P. HALVERSON[3,4]

[1]*Department of Earth and Planetary Sciences, Harvard University, Cambridge, MA 02138, USA*

[2]*School of Earth and Ocean Sciences, University of Victoria, Victoria, BC V8W 2Y2, Canada*

[3]*School of Earth and Environmental Sciences, The University of Adelaide, North Terrace, Adelaide, SA 5005, Australia*

[4]*Present address: Department of Earth and Plantary Sciences, McGill University, Montreal, QC H3A 2A7, Canada*

**Corresponding author (e-mail: paulfhoffman@yahoo.com)*

Abstract: In the Mackenzie Mountains, an arcuate foreland thrust-fold belt of Late Cretaceous–Paleocene age in the northern Canadian Cordillera, two discrete glacial–periglacial sequences of Cryogenian age (the Rapitan Group and the Stelfox Member of the Ice Brook Fm.) are separated by *c.* 1.0 km of non-glacial strata. The older Rapitan diamictite occurs in an amagmatic rift basin; the younger Stelfox diamictite occurs on a passive-margin continental slope.

The Rapitan Group consists of three formations. The lower Mount Berg Fm. is a complex of diamictites and conglomerates of limited extent. The middle Sayunei Fm. is a thick sequence of maroon-coloured mudrocks hosting innumerable graded layers of silt- and fine-grained sandstone. It lacks wave- or traction current-generated bedforms, and is lightly sprinkled with granule aggregates ('till pellets') and lonestones of dolostone and rare extrabasinal granitoids. It is capped by a hematitic Fe-formation that was reworked into the disconformably overlying Shezal diamictite. The Shezal Fm. is a complex of olive-green coloured boulder diamictites with subordinate, dark-grey shales, siltstones and parallel-sided sandstones. Some of the boulders are faceted and striated, and include dolostone, quartzite, siltstone and gabbro in declining order of abundance. Diamictite terminates abruptly at the top of the Shezal Fm., which is sharply overlain by dark shales or by $<$52 m of fetid, dark-grey, ^{13}C-depleted limestone with graded bedding.

The Stelfox Member is dominated by non-stratified, carbonate-clast diamictite with faceted and striated clasts, locally associated with subordinate, well-laminated shales containing till pellets and ice-rafted dropstones. It is thin or absent on the palaeocontinental shelf, but thickens seaward (southwestward) on the palaeocontinental slope. A thin clay drape separates it from a laterally continuous post-glacial 'cap' dolostone, which is a very pale coloured, micro- to macropeloidal dolostone with low-angle cross-laminae, giant wave ripples and local bioherms of corrugated stomatolites. In the NW, the dolostone is followed by reddish and greenish marls, followed by black shale of the Sheepbed Fm. In the SE, the dolostone is overlain by pink or grey limestones with well-developed sea-floor cements pseudomorphic after aragonite. In this area, the top of the dolostone is ferruginous and contains digitate rosettes of sea-floor barite cement, variably calcitized. The dolostone–limestone contact is perfectly conformable, and synclinal structures previously intepreted as karst features are tectonic in origin.

The grand mean palaeomagnetic pole for the well-studied Franklin Large Igneous Province (*c.* 718 Ma) of Arctic Laurentia, coeval with the basal Rapitan Group in the Mount Harper area, Yukon Territory, places the Mackenzie Mountains firmly in the tropics, at 18 $\pm$ 3°N palaeolatitude, at the onset of the Rapitan glaciation.

Carbon (δ^{13}C), oxygen (δ^{18}O) and strontium (^{87}Sr/^{86}Sr) isotopes have been measured in carbonates bracketing the Rapitan and Stelfox diamictites. Sulphur isotope data (δ^{34}S) have been obtained from carbonate-associated sulphate and barite above the younger diamictite, and calcium isotope data (δ^{44}Ca) from the younger carbonate itself. The results are broadly consistent with data from other areas. Iron isotope (δ^{57}Fe) and cerium anomaly (Ce/Ce*) values increase systematically upwards through the Sayunei Fe-formation, supporting an interpretation that deposition occurred within a redox chemocline through which the basin floor descended as a consequence of isostatic loading by the advancing Shezal ice sheet.

Supplementary material: Data are available at http://www.geolsoc.org.uk/SUP18470.

Glacial marine diamictites ('tillites') were recognized in the northwestern Mackenzie Mountains (Fig. 36.1) and to the west in the Yukon Territory by Shell Oil Company geologists in 1958 (Ziegler 1959), during the course of economic assessment of associated Fe-formations. At the time, they were thought to be early Palaeozoic in age (Ziegler 1959). They were referred to as the Rapitan Group by Green & Godwin (1963). Correlative strata were studied in the Hayhook Lake area (Fig. 36.1), 300 km to the SE, by Upitis (1966), Gabrielse *et al.* (1973), Young (1976) and Eisbacher (1978), where they were recognized as being of Neoproterozoic (Hadrynian) age. Gabrielse *et al.* (1973) erected a type section for the Rapitan Group near Hayhook Lake at 63°34'03"N, 127°02'41"W. It includes the Sayunei, Shezal and Twitya formations (Fig. 36.2). Eisbacher (1978) enlarged the Rapitan Group to include the Keele Fm. because of its gradational relationship with the Twitya Fm. However, Yeo (1981) and most subsequent workers follow the original definition (Green & Godwin 1963) and limit the Rapitan Group to glaciogenic strata beneath the Twitya Fm. Additional stratigraphic and sedimentological studies of the Rapitan Group along the 400 km arc of the Mackenzie Mountains were carried out by Eisbacher (1981*a*, *b*, 1985) and Yeo (1981, 1984, 1986).

A second, thinner, glaciogenic unit was discovered $>$1000 m stratigraphically above the Rapitan Group by Aitken (1991*a*, *b*). He defined it as the Stelfox Member ($<$272 m) of the Ice Brook Fm., the type section of which is located in the Sayunei Range at 64°08′07″N, 129°00′38″W (Aitken 1991*b*). It is overlain by a distinctive carbonate unit, the 'Tepee dolostone' of Eisbacher (1978, 1981*a*) and Aitken (1991*b*), subdivided into the Ravensthroat and Hayhook formations by James *et al.* (2001). The dolomite features unusual sedimentary structures, including sheet-crack cements, reverse-graded peloids, giant wave ripples, corrugated stromatolites and sea-floor cements (crystal fans) originally composed of aragonite and barite (Eisbacher 1981*a*; Aitken 1991*b*; James *et al.* 2001; Hoffman & Schrag 2002; Allen & Hoffman 2005; Hoffman & Macdonald 2010). It has many similarities with post-glacial cap dolostones on other palaeocontinents (Hoffman *et al.* 2011), which allow the base of the Ediacaran Period to be recognized globally (Knoll *et al.* 2006).

Correlatives of the Mackenzie Mountains and Windermere supergroups, including both glacial horizons, are discontinuously exposed in Wernecke and Ogilvie in central Yukon Territory (Macdonald & Roots 2009; Macdonald *et al.* 2010*b*), and in the Tatonduk inlier of east-central Alaska (Young 1982; Macdonald *et al.* 2010*a*; Macdonald & Cohen 2011).

From: ARNAUD, E., HALVERSON, G. P. & SHIELDS-ZHOU, G. (eds) *The Geological Record of Neoproterozoic Glaciations*. Geological Society, London, Memoirs, **36**, 397–411. 0435-4052/11/$15.00 DOI: 10.1144/M36.36

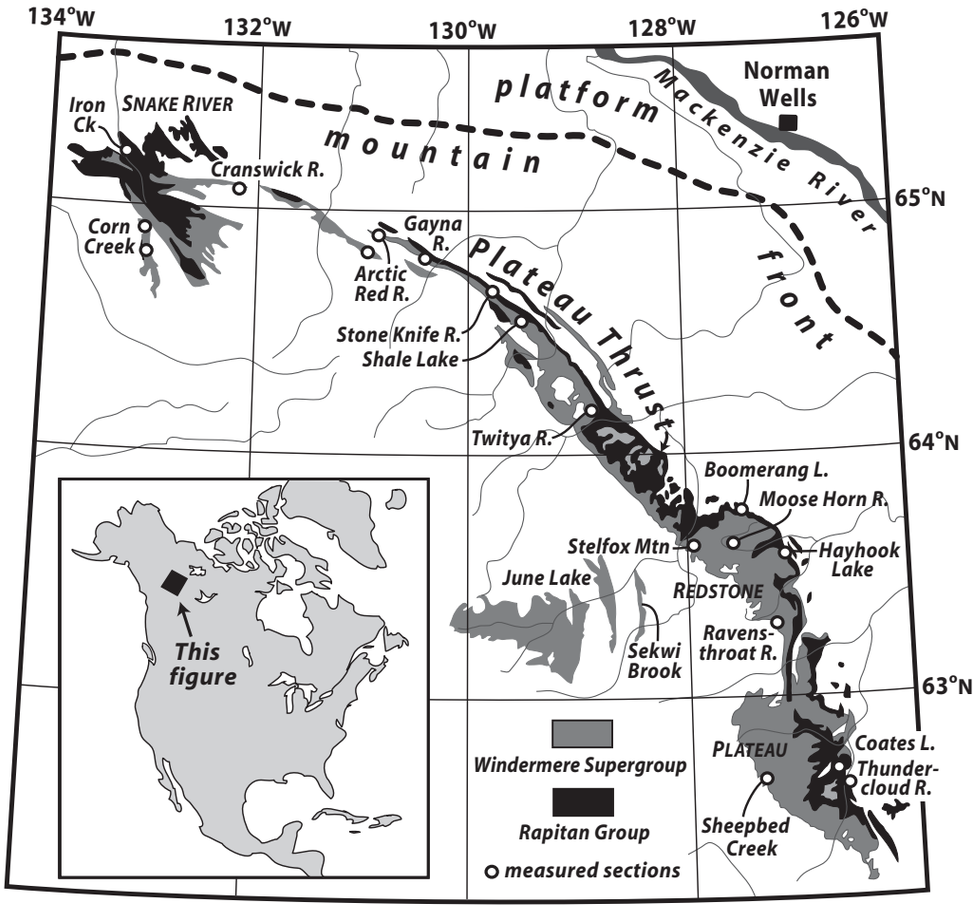

Fig. 36.1. Outcrop distribution of the Rapitan Group and the Windermere Supergroup in the Mackenzie Mountains, showing locations of measured sections forming the basis of this report.

This chapter is a synopsis of previous work, augmented by seven new sections of the Rapitan Group, measured by P.F.H. in the Iron Creek (65°03′15″N, 133°07′31″W: >775 m), Gayna River (64°49′23″N, 130°27′11″W: 22 m), Stone Knife River (64°41′53″N, 129°53′19″W: 114 m), Shale Lake (64°32′41″N, 129°22′37″W: 995 m), Boomerang Lake (63°46′46″N, 127°28′05″: >236 m), Hayhook Lake (63°34′38″N, 127°05′34″W: 997 m) and Ravensthroat River (63°13′57″N, 127°03′18″W: 230 m) areas; and 13 sections of the Stelfox diamictite (all <35 m) and its post-glacial carbonate sequence at Cranswick River (65°05′54″N, 132°26′17″W), Arctic Red River (64°56′05″N, 131°03′30″W), Gayna River (64°49′22″N, 130°28′27″W), Stone-knife River (64°40′36″N, 129°53′48″W), Shale Lake (64°31′12″N, 129°29′09″W), Twitya River (64°13′07″N, 128°38′11″W), Moose Horn River (63°57′13″N, 127°30′39″W), Hayhook Lake (63°34′17″N, 127°11′44″W), Stelfox Mountain (63°36′01″N, 127°50′47″W; 63°35′46″N, 127°53′04″W; 63°35′60″N, 127°53′57″W; 63°35′37″N, 127°55′11″W) and Ravensthroat River (63°17′05″N, 127°08′40″W). The named locations are indicated in Figure 36.1. The coordinates refer to the base of the section.

Group	Formation	Member	Reference
	Sheepbed		Gabrielse *et al.* (1973)
	Hayhook		James *et al.* (2001)
	Ravensthroat		
	Ice Brook	▼ Stelfox ▼	Aitken (1991b)
		Delthore	
		Durkan	
	Keele		Eisbacher (1978)
	Twitya		
Rapitan	▼ Shezal ▼		
	▼ Sayunei ▼		
	▼ Mt Berg ▼		
Coates Lake	Copper Cap		Gabrielse *et al.* (1973)
	Redstone River		
	Thundercloud		Jefferson (1983)
Little Dal			Aitken (1981)

Fig. 36.2. Stratigraphic nomenclature and defining references for units associated with Cryogenian glaciogenic strata (black with inverted triangles) in the Mackenzie Mountains.

Structural framework

The Mackenzie Mountains are the physiographic expression of an arcuate, NE-vergent, foreland thrust–fold belt of Late Cretaceous–Paleocene age in the northern Canadian Cordillera (Aitken & Long 1978; Aitken 1982; Narbonne & Aitken 1995). Late Neoproterozoic strata of the Windermere Supergroup (Fig. 36.3) are principally exposed in the hanging wall of the Plateau Thrust system (Fig. 36.1). Their subhorizontal (Redstone Plateau) or SW-dipping attitude depends on their position above a flat or ramp in the thrust plane. Outcrop-scale strain is heterogeneous; structurally intact, low-strain sections can be located by

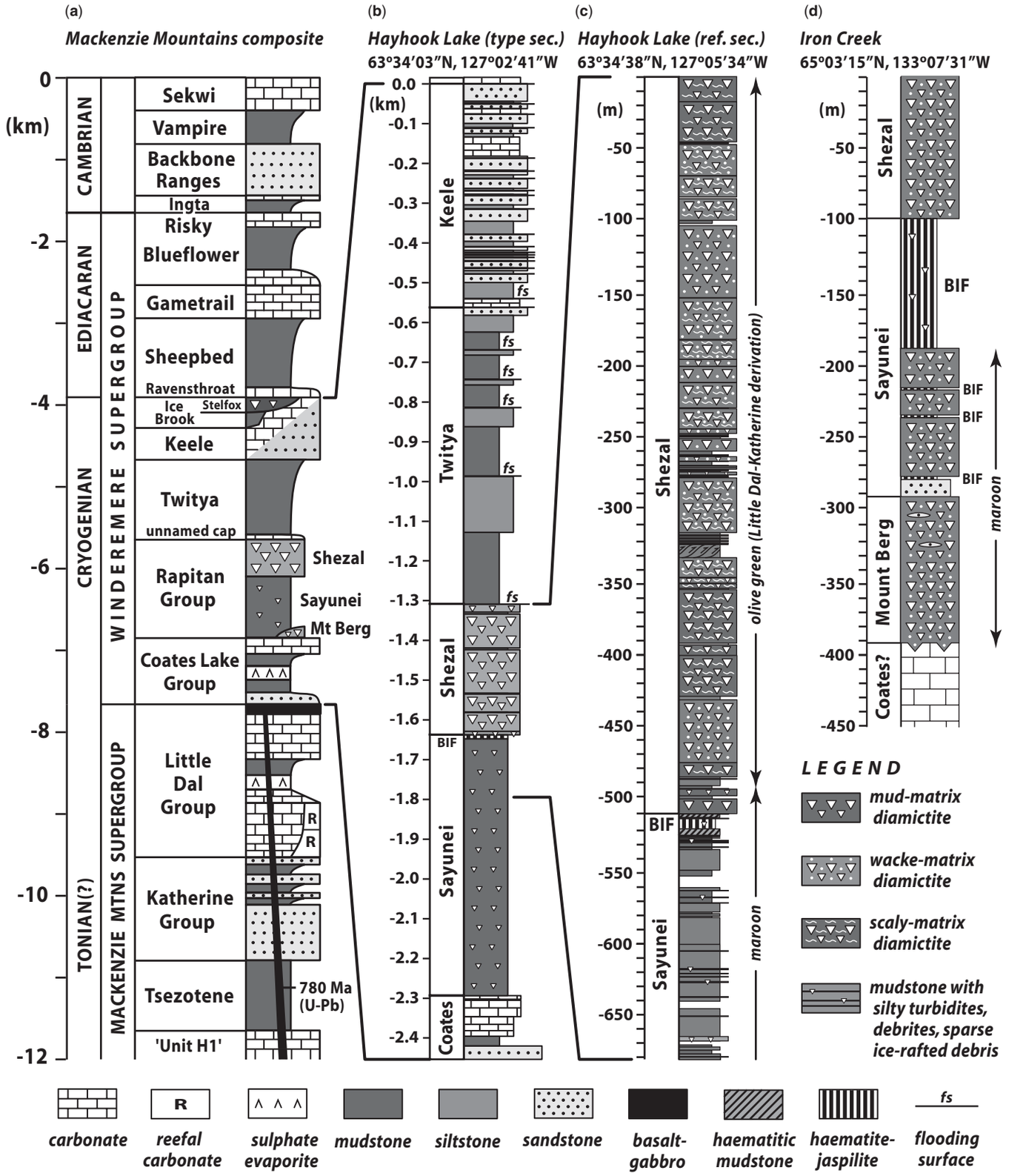

Fig. 36.3. (**a**) Composite columnar section of Neoproterozoic strata in the Mackenzie Mountains (modified after Narbonne & Aitken 1995). (**b**) Type section of the Rapitan Group (Gabrielse *et al.* 1973) in the Hayhook Lake area (see Fig. 36.1 for location) as remeasured by P.F.H. (**c**) Detailed section of the upper Sayunei and Shezal formations 1.6 km NW of the Rapitan Group type section. Note Fe-formation ('BIF') at the top of the Sayunei Formation, representing 'basin-facies' Fe-formation (Eisbacher 1985). (**d**) Section of the lower Rapitan Group near Iron Creek, representative of 'transitional-facies' Fe-formation (Eisbacher 1985).

mapping. Long slopes are unattractive because of scree. Published 1:250 000-scale map coverage is incomplete and stratigraphically inconsistent.

An unconformity at the base of the Backbone Ranges Fm. (Early Cambrian) cuts progressively down-section from SW to NE, with the result that the Windermere Supergroup is missing to the NE of

the Plateau Thrust system. To the SW, the glaciogenic units are buried by younger strata. Although the outcrop belt of Windermere strata is less than 30 km wide, it fortuitously preserves the outer shelf-edge and upper slope of a continental terrace developed in late Cryogenian (Keele Fm.) to early Ediacaran (Sheepbed Fm.) time (Ross 1991; Narbonne & Aitken 1995; Dalrymple & Narbonne 1996; Day *et al.* 2004). Continental rifting, leading to the formation of the continental terrace, controlled sedimentation during the Coates Lake and Rapitan groups (Eisbacher 1981*a*, 1985; Jefferson 1983), as well as during the preceding Mackenzie Mountains Supergroup (Turner & Long 2008). The Coates Lake and Rapitan basins are interpreted by Jefferson & Ruelle (1986) and Yeo (1981), respectively, as rhombochasms ('pull-apart' basins) associated with hypothetical strike–slip systems, systems that are not mutually compatible in orientation.

Stratigraphy

Mackenzie Mountains Supergroup

The Mackenzie Mountains Supergroup is a broadly conformable succession composed of sandstone, siltstone, carbonate and evaporite of mostly shallow-marine origin (Fig. 36.3a). Its upper part, the Little Dal Group, is 2 km thick in its type section (Gabrielse *et al.* 1973; Aitken 1981; Halverson 2006) and is dominated by carbonate with a recessive interval of gypsiferous siltstone. The carbonates are platformal in the SE and basinal in the NW, with reefal build-ups in the lower part (Aitken 1981; Turner *et al.* 1997). The carbonate is conformably overlain by and locally interstratified with pillow basalt, the Little Dal lavas of Aitken (1982). These are possibly the extrusive equivalents of the Tsezotene dykes and sills (Aitken 1982), which belong to the 780 Ma Gunbarrel large igneous province (Harlan *et al.* 2003).

Coates Lake and Rapitan groups

The Coates Lake Group is an assemblage of sandstone, carbonate-clast conglomerate, gypsiferous siltstone and carbonate, including fetid basinal limestone with turbidites and 'debrites' (i.e. coarse-grained mass-flow deposits) (Ruelle 1982; Jefferson & Ruelle 1986). The Rapitan Group (Eisbacher 1978, 1981*a*) includes the Sayunei (sigh-YOU-knee) Fm., composed of maroon coloured, subaqueously deposited, fine-grained clastics with subordinate debrites and lonestones, and the overlying Shezal (shiz-ALL) Fm., a stack of mostly olive-coloured, polymictic 'diamictites' (i.e. massive, foliated or bedded wackestone with randomly dispersed, matrix-supported pebbles and boulders, characteristically faceted and striated) with thin interbeds of dark shale and sandstone. Locally, an older diamictite complex (Mount Berg Fm.) occurs below the Sayunei Fm. (Yeo 1981). The Rapitan Group onlaps tilted Coates Lake and Little Dal group strata unconformably (Eisbacher 1978, 1981a, 1985). Basinal facies of the Coates Lake Group are black, pyritic and organic-rich; those of the Rapitan Group are maroon, hematitic and organic-poor.

Twitya, Keele and Ice Brook formations

A major marine transgression followed the Rapitan glaciation, providing accommodation for 330–765 m of dark grey shale, siltstone and fine-grained sandstone of the Twitya Fm. (Eisbacher 1978, 1981*a*; Aitken 1982). Resting sharply upon boulder diamictite of the upper Shezal Fm., at the base of the Twitya Fm., are 0–52 m of dark-grey, thin-bedded limestone (Eisbacher 1978, 1981*a*; Aitken 1982), which are absent in the Rapitan Group type section (Hayhook Lake) and thickest at Shale Lake (Fig. 36.1). Above the Twitya Fm. lie 220–600 m of cyclic, shallow-marine sandstone, siltstone, limestone and dolomitized limestone of the Keele Fm. (Day *et al.* 2004). A thin, jasper-pebble conglomerate occurs widely near its base. Glendonites, interpreted as pseudomorphs after ikaite ($CaCO_3{\cdot}6H_2O$), occur close to the same horizon (James *et al.* 2005).

The outer edge of the Keele platform is exposed near Shale Lake and on Stelfox Mountain (Fig. 36.1), where a SW-dipping 'breakaway scarp' (Aitken 1991*b*, p. 26) separates shallow-marine Keele strata on the footwall from hotel-size megaclast breccia (Durkan Member), turbiditic siltstone (Delthore Member) and glaciogenic diamictite (Stelfox Member) of the Ice Brook Fm. on the hanging wall (Aitken 1991*b*; Shen *et al.* 2008). The Stelfox diamictite is buttressed against the palaeoscarp and its feather-edge steps across the trace of the palaeoscarp on Stelfox Mountain (at 63°35′58″N, 127°52′02″W) onto the Keele Formation of the footwall (Fig. 36.4b). The Ravensthroat Fm. passes across the fault line without displacement, proving that movement on the palaeoscarp ended before the glacial termination. Eisbacher (1981*a*) inferred that the Durkan megabreccia was triggered by glacioeustatic fall, but this interpretation was rejected by Aitken (1991*b*), who argued that pore-fluid overpressures would not develop in unconsolidated sediments unless the base-level fall was catastrophically rapid. He (Aitken 1991*b*) insisted that only the Stelfox Member was glacial in origin. P.F.H. therefore prefers the name Stelfox glaciation over Ice Brook glaciation, despite the latter's priority in the literature (Kaufman *et al.* 1997).

Ravensthroat, Hayhook and Sheepbed formations

As with the Rapitan glaciation, major marine flooding followed by Stelfox diamictite deposition, providing accommodation on the Keele platform for the formation of a transgressive, post-glacial carbonate (Raventhroat/Hayhook formations) and 446–562 m of black shale and minor siltstone of the Sheepbed Fm. (Pyle *et al.* 2004; Shen *et al.* 2008). On the continental slope SW of the Keele platform, the Sheepbed Fm. reaches 1050 m in thickness at Sekwi Brook (Fig. 36.1) and includes significantly more siltstone, deposited by both turbidity flows and unidirectional (NW-directed) contour currents (Dalrymple & Narbonne 1996). The contourites are estimated to have formed in water depths of 1.0–1.5 km and imply that the slope was open to the world ocean in a gulf >100 km wide (Dalrymple & Narbonne 1996).

Glaciogenic and associated strata

Rapitan Group

The remeasured type section of the Rapitan Group (Gabrielse *et al.* 1973) is shown in Figure 36.3b. The Sayunei Fm. (487 m) consists of maroon-coloured mudstone with innumerable graded beds of siltstone and/or fine-grained sandstone, some with outsized clasts of dolostone. Granule- to small pebble-sized lonestones are sprinkled throughout the mudstone. The clasts are commonly rimmed by chlorite, formed by reaction between the dolostone and the host mudstone. Some clasts are aggregates of sand or granules, interpreted as 'till pellets' (Ovenshine 1970) by Young (1976) and Eisbacher (1981*a*). Bedforms attributable to wave action are absent, as is evidence of bottom traction currents. Greenish mudstone beds occur, but none are dark grey or black, in stark contrast to the basinal facies of the underlying Coates Lake Group.

In the Hayhook Lake area (Fig. 36.1), the top of the Sayunei Fm. is marked by 10–16 m of brick-red, hematitic mudstone and hematite jaspilite (Fig. 36.3c). This interval is parallel-laminated and lacks evidence for bottom traction currents. Within the Fe-rich formation are lonestones and thin dolostone-clast debrites (Young 1976). The former include rounded cobbles and small boulders of porphyritic quartz monzonite (i.e. two-feldspar

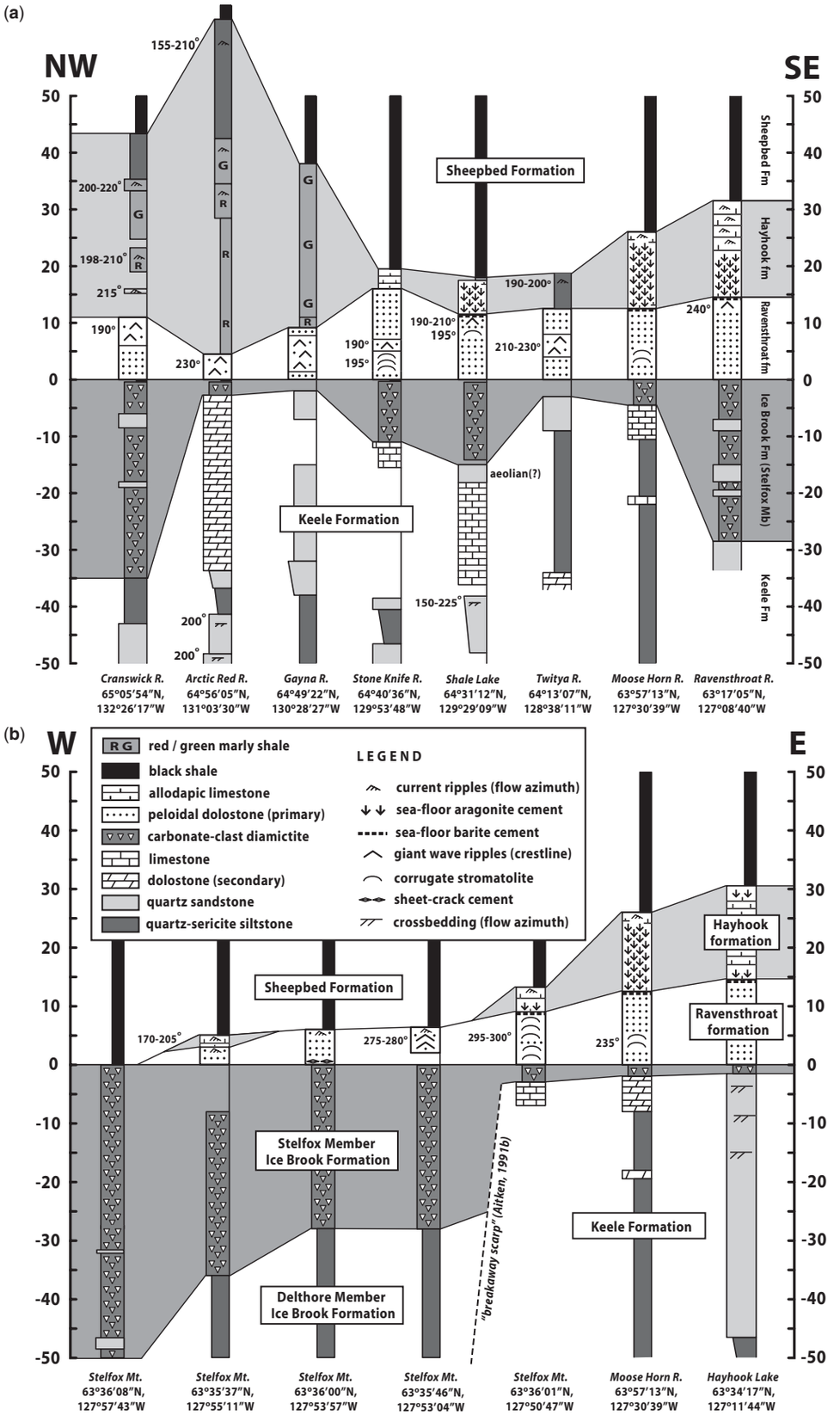

Fig. 36.4. Stratigraphic relations based on columnar sections spanning the Stelfox Member and its post-glacial carbonate sequence (Raventhroat and Hayhook formations) in lines oriented parallel (**a**) and transverse (**b**) to the depositional strike of the Neoproterozoic passive margin. The 'breakaway scarp' (Aitken 1991*b*) marks the outer edge of the Keele Formation shelf. Megaclast breccia of the Durkan Member (not shown) conformably underlies the Delthore Member and both abut the 'breakaway scarp' at a buttress unconformity.

granitoid with 5–15% quartz). The Fe-formation is overlain disconformably by maroon-coloured diamictite (basal Shezal Fm.), which contains rounded and angular clasts from the lower unit. In some sections, the Fe-formation is missing and was probably removed by erosion at the base of the Shezal Fm.

In the Iron Creek area (Fig. 36.3d), an aggregate thickness of 100–120 m of hematite jaspilite with pea-sized jasper nodules (mini-concretions) is sandwiched between units of poorly stratified, boulder diamictite with subordinate beds and lenses of tabular cross-bedded, medium-grained, well-rounded, monocrystalline, quartz

sandstone (Yeo 1981, 1986; Klein & Beukes 1993). Outsized clasts and debrites occur within the jaspilite intervals, as do thin seams and lenses of Fe-carbonate (siderite). The Hayhook Lake area and Iron Creek sections represent respectively the 'basinal' and 'transitional' (more proximal) facies of Fe-formation distinguished in the Rapitan Group by Eisbacher (1985).

The Shezal Fm. diamictite is mostly olive-green or grey in colour, except for the basal part, which is maroon and clearly derived from the underlying Sayunei Fm. (Fig. 36.3c). The clasts consist of dolomite (Little Dal Group), commonly stromatolitic, quartzite (Katherine Group), siltstone (Coates Lake Group and Tsezotene Fm.), basalt and gabbro. Extrabasinal clasts are rare. Faceted and striated clasts, particularly siltstone, are abundant and unequivocally glacial in origin (Young 1976; Eisbacher 1981*a*). Diamictite occurs in crudely tabular, poorly stratified, matrix-supported bodies up to 90 m thick. The matrix consists variably of wackestone, structureless mudstone, or mudstone with anastomosing ('scaly') foliation (Fig. 36.3c) that is subparallel to bedding but unrelated to the axis of maximum tectonic compression. The Shezal Fm. (320 m thick) is unusually well-exposed in a river canyon 1.6 km NW of the type area (Fig. 36.3c), where diamictite units are separated by subordinate, recessive intervals of well-stratified siltstone, graded sandstone and dark-grey shale. A 6-m-thick duplex structure with thrusting directed toward the NE occurs in the reference section between −320 and −330 m (Fig. 36.3c). In this section, the tops of the diamictite bodies tend to be more sharply defined than their bases.

No post-glacial carbonate is present in the type section of the Rapitan Group (Fig. 36.3b), but elsewhere the basal Twitya Fm. consists of thin graded beds of dark-grey, allodapic limestone (Eisbacher 1978, 1981*a*; Aitken 1982). The carbonate reaches a thickness of 52.5 m at Shale Lake. At Stone Knife River (Fig. 36.1), where 40 m of limestone is exposed, its lower part is hummocky cross-stratified. Near Corn Creek (Fig. 36.1), bordering the Wernecke Mountains, up to 300 m of massive dolomite (Mount Profeit Fm.) is laterally equivalent to the lower Twitya post-glacial limestone (Eisbacher 1981*a*).

Stelfox Member (Ice Brook Fm.)

Whereas the Rapitan Group is up to 1500 m thick (Yeo 1981), the Stelfox Member is less than 40 m thick in most sections (Fig. 36.4) and the thickest, 308 m (Atiken 1991*a*), is also the deepest-water section of Stelfox diamictite in the Mackenzie Mountains. Basinward thickening could account for the modest thickness of the Stelfox diamictites, which are only preserved in shelf and upper-slope settings, in contrast to the deep rift-basin setting of the Rapitan Group.

At Shale Lake (Fig. 36.4a), the Stelfox diamictite is directly underlain by 5–9 m of well-sorted, well-rounded, medium-grained, quartz sandstone of possible aeolian origin. Large-scale tabular cross-bedding indicates transport to the SSW (*c.* 205° azimuth, $n = 2$), consistent with easterly palaeowinds (see below). The presence of aeolianite beneath the diamictite would suggest that glacioeustasy preceded or outranked glacioisostasy.

The Stelfox Member is typically recessive and masked by scree from the overlying Ravensthroat Fm., which along with its modest thickness accounts for its delayed recognition. The dominant lithology is massive to weakly stratified diamictite, in which rounded clasts of tan dolostone and grey limestone are supported by a matrix of brownish-tan carbonate-rich mudrock with dispersed grains of quartz sand and granules. The clasts are derived from the underlying Keele Fm. and the absence of quartzite clasts suggests that carbonates were the only components of the Keele Fm. that were strongly lithified at the time of glaciation. Beds and lenses of quartz-chert sandstone, micaceous wacke and polymictic debrite are subordinate components of the Stelfox Member. At Cranswick River section (Fig. 36.4a), the diamictite has a terrigenous matrix and the carbonate clasts, freed in float, are visibly faceted and striated. Ice-rafted dropstones and 'till pellets' (Ovenshine 1970) are well-developed in laminated facies (Aitken 1991*a*, *b*).

Ravensthroat–Hayhook post-glacial carbonate couplet

The Stelfox diamictite or its equivalent erosion surface is everywhere sharply overlain by a transgressive, 10–15-m-thick, cap dolostone (Fig. 36.4), previously known informally as the 'Tepee dolostone' (Eisbacher 1981*a*, 1985; Aitken 1991*b*). The pale, incandescent, yellowish-grey scree profusely generated by the informally defined Ravensthroat Fm. (James *et al.* 2001) could not be more unlike the jet-black feathers of its avian namesake. East of 130°W longitude, the dolostone is overlain by up to 15 m of ledge-forming grey or pink limestone (Fig. 36.4), informally defined as the Hayhook Fm. (James *et al.* 2001). West of 130°W longitude, it is overlain by an ascending sequence of red, green and grey shales with thin beds of current-rippled limestone (Fig. 36.4). This tri-coloured sequence is remarkably similar to that overlying the homologous postglacial cap dolostones (Hambrey & Spencer 1987; Halverson *et al.* 2004) in East Greenland (e.g. Kap Weber, Andrée Land) and East Svalbard (e.g. Ditlovtoppen, Ny Friesland).

The Ravensthroat Fm. consists of micro- and macropeloidal dolostone with ubiquitous, low-angle, cross-lamination defined by normal and reverse-graded laminae (James *et al.* 2001). The peloids are structureless, sub-spherical aggregates of dolomicrite up to 3 mm in diameter. They commonly rest on abraded facets. Giant wave ripples (cf. Allen & Hoffman 2005) are well developed in many sections (Fig. 36.4). They are trochoidal in profile, with sharp crests and lobate troughs, and individual ripple trains aggrade for up to 1.4 m through bidirectional accretion of peloidal laminae. Their synoptic relief, crest to trough, is up to 40 cm. The structures are different in form and origin from peritidal 'tepees' (Assereto & Kendall 1977; Kendall & Warren 1987); they are not brecciated, lack syndepositional cements, and their crestlines are linear and parallel, not polygonal, in plan view (Eisbacher 1981*a*; Aitken 1991*b*; James *et al.* 2001). Their crestlines generally trend NE, at a high angle to the Keele shelf edge (Fig. 36.5).

Decametric bioherms composed of corrugated stromatolites (James *et al.* 2001) oriented subparallel to the crests of giant wave ripples occur in some sections (Fig. 36.4). The corrugated

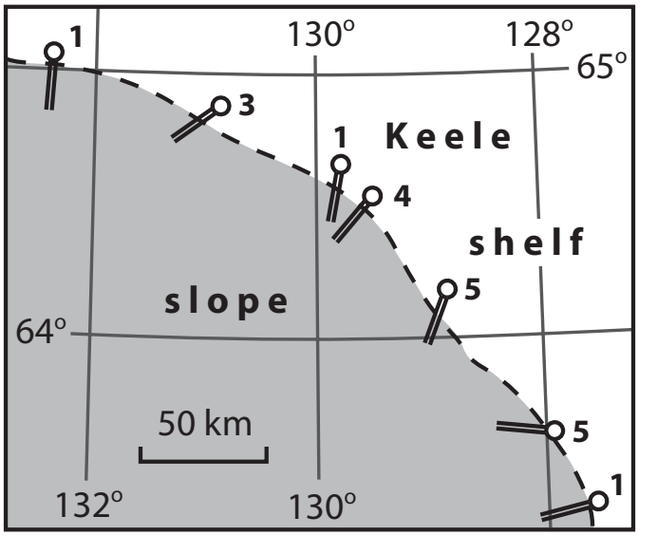

Fig. 36.5. Mean orientations of crestlines (double bars) of giant wave ripples in the Ravensthroat Fm. at different locations. Numerals are the numbers of independent ripple trains measured at each location.

stromatolites are closely similar to those that are intergradational with 'tubestone' stromatolites in the homologous Keilberg cap dolostone in northern Namibia. Evidence of subaerial exposure is absent, but there can be no doubt that the Ravensthroat Fm. was deposited above wave-base and within the euphotic zone.

In virtually all sections from Shale Lake to Ravensthroat River (Fig. 36.1), a distance of nearly 200 km, the uppermost 4–10 cm of the Ravensthroat Fm. contains a remarkable digitate crust composed of sea-floor barite ($BaSO_4$) cement, variably pseudomorphosed by calcite. At Shale Lake, the barite crust is developed directly on a train of giant wave ripples. Because of pseudomorphic replacement in some sections, the barite cement was formerly misinterpreted as an aragonite cement (Aitken 1991*b*, fig. 8) or as microdigitate stromatolites (James *et al.* 2001, fig. 10). The digits consist of rosettes or bundles of bladed crystals whose morphology is quite distinct from the prismatic (pseudohexagonal) habit of the former aragonite cements in the overlying Hayhook Fm. (James *et al.* 2001). The digits preserve growth lamellae, 1–2 mm thick, and typically tilt to the SW due to preferential growth in the seaward direction. The spaces between the digits are filled by laminated, peloidal, ferroan dolomite, the dark brown colour of which contrasts with the pale colouration of the rest of the Ravensthroat Fm. The borders of the barite digits are ragged due to the growth of vertically standing barite crystals that lap out onto the upper surfaces of individual laminae of infilling peloidal dolomite. This provides textural proof that the barite digits formed simultaneously with the peloidal infills. This interpretation agrees with that of barite cements at the homologous post-glacial dolostone–limestone transition in central Australia (Kennedy 1996).

The tips of the barite digits, marking the Ravensthroat–Hayhook transition, are typically 'colonized' by slender prismatic fans of pseudomorphosed aragonite, while at the same level the peloidal ferroan dolostone changes to calcimicrite, initially with some reworked dolostone. Locally, the barite crust was dissolved away instead of pseudomorphically replaced, and the barite cement layer is represented by a collapse microbreccia of ferroan dolostone clasts, overlain by calcimicrite of the basal Hayhook Fm.. The local occurrence of this microbreccia contributed to the misinterpretation of the contact as a karstic unconformity (James *et al.* 2001, fig. 9B).

Numerous mesoscopic folds at the Ravensthroat–Hayhook contact, previously interpreted as karst channels (James *et al.* 2001, fig. 9A), are consistently oriented parallel to tectonic cleavage and regional folds. They are not karst channels because the primary stratification in both units is everywhere parallel to the contact. We interpret them as lobate-cuspate folds (Ramsay & Huber 1987) of tectonic origin and Late Cretaceous–Paleocene age, related to bedding-parallel shortening at the rheological interface between the stiff Ravensthroat dolostone and the weak Hayhook limestone. Contrary to James *et al.* (2001), we find no evidence of karstic unconformity, subaerial exposure or isostatic adjustment at the Ravensthroat–Hayhook contact.

The Hayhook Fm. is 0–15 m thick (Fig. 36.4) and consists of flaggy micrite with pseudomorphosed crystal fans of aragonite cement (James *et al.* 2001). The cement fraction generally increases upward and reaches nearly 100% in some sections, notably Shale Lake (Fig. 36.1). The detailed interplay between cement growth, burial by micrite and renewed cement development indicates precipitation at a free-face on the sea-floor.

Boundary relations with overlying and underlying non-glacial units

Rapitan Group

A low-angle unconformity separates the glaciogenic Rapitan Group from various units of the underlying Coates Lake and Little Dal groups (Gabrielse *et al.* 1973; Eisbacher 1978, 1981*a*, 1985; Aitken 1982; Jefferson & Ruelle 1986). In the Hayhook Lake area (Fig. 36.1), the Coates Lake Group is onlapped by the Sayunei Fm. along the unconformity (Eisbacher 1978, 1981*a*). The presence of submarine carbonate-clast talus breccias in the lower Rapitan Group (beneath and within the lower Sayunei Fm.) on the northeastern margin of the outcrop belt near Shale Lake (64°32′41″N, 129°22′37″W) suggests a master normal fault on that side of the basin. It may have been structurally inverted during orogenic contraction to form a part of the Plateau Thrust system. The maroon colour of the Sayunei stems in part from its derivation from the Coates Lake Group, which is dominated by reddish siltstones of the Redstone River Fm. Similarly, the olive-green colouration of the overlying Shezal diamictites reflects its derivation from the grey carbonates and greenish basalts of the Little Dal Group.

A knife-sharp, marine, flooding surface separates the Shezal Fm. from fetid, dark-grey, flaggy limestone and shale of the lower Twitya Fm. (Eisbacher 1978, 1981*a*). Where the Rapitan Group is absent, the Twitya transgresses older units disconformably (Narbonne & Aitken 1995).

Stelfox Member

A low-angle unconformity (Fig. 36.4a) separates the Stelfox diamictite from shelf carbonates and clastics of the underlying Keele Fm. (Day *et al.* 2004). West of the palaeoscarp at Stelfox Mountain (Fig. 36.4b), a sharp disconformity separates the Stelfox diamictite from parallel-laminated, greenish-grey siltstone of the underlying Delthore Member (Aitken 1991*b*). As the Delthore Member was deposited below storm wave-base, glacial erosion may be required to account for the sharp disconformity.

A major marine flooding surface separates the Stelfox Member, or the Keele Fm. where the Stelfox is absent, from the overlying Ravensthroat Fm. Where the basal contact of the dolostone is not covered by its own scree (e.g. Cranswick River, Arctic Red River, Stoneknife River), 10–20 cm of clay separate it from the underlying diamictite.

The top of the Hayhook limestone is a conformable marine flooding surface overlain by organic-rich black shale of the Sheepbed Fm. (Pyle *et al.* 2004; Shen *et al.* 2008).

Chemostratigraphy

Carbon isotopes

Carbon-isotopic records have been published for the Little Dal and Coates Lake groups (Halverson 2006), the Twitya post-glacial limestone and Keele Fm. (Narbonne *et al.* 1994; Kaufman *et al.* 1997; Hoffman & Schrag 2002), and the Ravensthroat–Hayhook post-glacial carbonate (James *et al.* 2001). The Little Dal Group is enriched in ^{13}C relative to the PDB standard, except for a depleted interval in the Upper Carbonate Fm. The overlying Coates Lake Group begins with a deep negative excursion to −8‰ in $\delta^{13}C$, followed by a positive excursion to +8‰ before settling back to modestly enriched values.

Values of $\delta^{13}C$ in the Twitya post-glacial limestone increase up-section from −2.5‰ at the base. Carbonates of the Keele Fm. are strongly enriched, $\leq +8$‰, but plunge to −8‰ in the last 30 m of section beneath the Stelfox diamictite.

The Ravensthroat Fm. is also depleted in ^{13}C (Fig. 36.6) and values decline up-section. The Ravensthroat–Hayhook contact coincides with a −2‰ step function. This is broadly consistent with low-temperature equilibrium fractionation between dolomite and calcite (Friedman & O'Neil 1977). Within the Hayhook Fm., $\delta^{13}C$ rises by *c.* 1‰ up-section, with no systematic difference in values between micro-drilled micrite and sea-floor cement (Fig. 36.6).

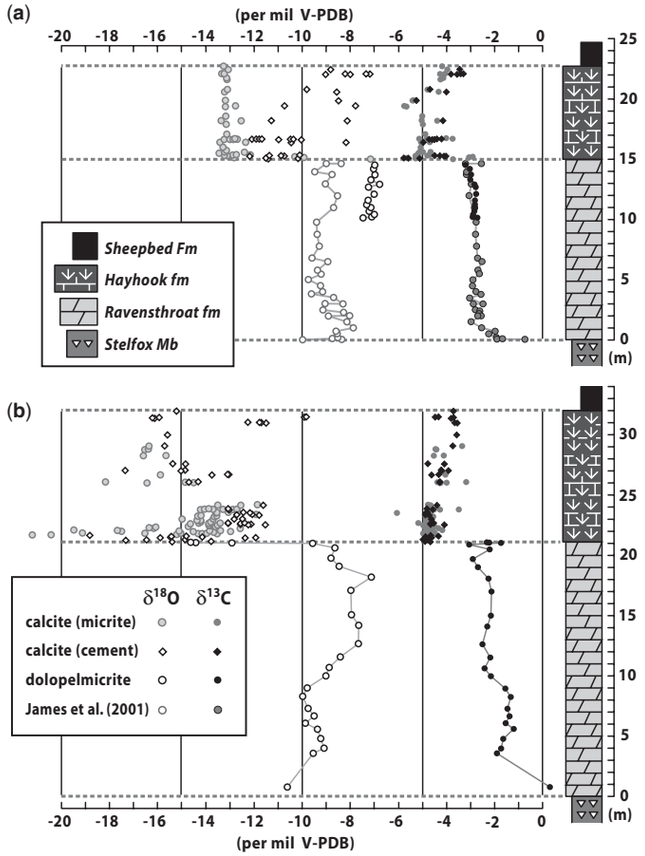

Fig. 36.6. C- and O-isotope data from dolomite of the Ravensthroat Fm. and from coexisting micrite and sea-floor cement of the Hayhook formation at (**a**) Shale Lake and (**b**) Ravensthroat River.

Oxygen isotopes

In order to test the possibility of low-temperature dolomite–calcite equilibrium fractionation, which would imply a sea-floor origin for the Ravensthroat dolomite, and also for the possibility that the Hayhook sea-floor cements and associated micrites might retain a record of bottom and surface waters, respectively, we plot unpublished O-isotope data for two sections that we sampled in detail (Fig. 36.6). Exceptional petrographic preservation of the sea-floor cements motivated this effort. At Shale Lake, the Ravensthroat-Hayhook contact coincides with a −6‰ step function in $\delta^{18}O$, taking the micritic component to be representative of the surface waters, from which the Ravensthroat was also derived (Fig. 36.6a). The magnitude of the step function in $\delta^{18}O$, roughly 3× that in $\delta^{13}C$, is compatible with a low-temperature equilibrium fractionation between dolomite and calcite (Friedman & O'Neil 1977).

The sea-floor cements are consistently more enriched in ^{18}O than the micritic component of the Hayhook (Fig. 36.6a), consistent with lower temperatures and/or higher salinities of the bottom waters, from which the cements were precipitated, relative to the surface waters. The cements become more enriched in ^{18}O up-section (Fig. 36.6a), which could indicate an increase in the temperature and/or salinity gradient, or alternatively an increase in water depth, with time. The cements exhibit considerably more scatter in $\delta^{18}O$ than does the micrite, which could reflect the difficulty in micro-drilling cement without contamination from the micrite that fills in between the slender prisms of former aragonite and even their originally hollow interiors. Accordingly, the reduction in scatter towards the top of the Hayhook reflects the more massive and continuous nature of the uppermost cements.

An alternative, less consequential, interpretation of the $\delta^{18}O$ data is that the micrite was preferentially altered by diagenetic fluids on account of its finer grain size compared with the cements, and therefore its greater surface-to-volume ratio. The $\delta^{18}O$ data are more depleted in ^{18}O and display more scatter in the second section (Fig. 36.6b), at Ravensthroat River. This section illustrates the ease with which $\delta^{18}O$, but not $\delta^{13}C$, was diagenetically altered.

Strontium isotopes

New and previously published (Kaufman *et al.* 1993, 1997) $^{87}Sr/^{86}Sr$ data from Sr-rich (300–3000 ppm), low-Mn ($Mn/Sr < 0.1$) limestones bracketing the Rapitan and Stelfox glaciations in the Mackenzie Mountains are given in Halverson *et al.* (2007). Non-radiogenic values of 0.70550–0.70622 ($n = 10$) are observed in the Little Dal Group, compared with 0.70644–0.70669 ($n = 5$) in the Coates Lake Group. No data are currently available for the post-Rapitan limestone (basal Twitya Fm.), but limestones directly beneath the Stelfox diamictite (uppermost Keele Fm.) have ratios of 0.70718–0.70720 ($n = 3$). Sea-floor cements from the Hayhook post-glacial limestone are marginally less radiogenic at 0.70714–0.70716 ($n = 4$) than the Coates Lake Group, whereas the coexisting micrites are more radiogenic, with minimum values of 0.70751–0.70792 ($n = 5$), which is consistent with preferential alteration. All reported Hayhook values are from samples with Sr concentrations >600 ppm and $Mn/Sr < 0.1$.

Sulphur isotopes and iron speciation

Sulphur isotopes have been measured from carbonate-associated sulphate in the Ravensthroat and Hayhook formations, as well as from the barite sea-floor cement at the top of the Ravensthroat Fm. (M.T. Hurtgen, pers. comm. 2008). The $\delta^{34}S_{CAS}$ and $\delta^{34}S_{barite}$ values are mutually consistent and agree with values from correlative strata in Namibia (Hurtgen *et al.* 2006), but the data have yet to be published.

Sulphide S isotopes and Fe-speciation (ratio of highly reactive Fe to total Fe) have been studied in organic-rich black shales of the Sheepbed Fm. (Fig. 36.3) in order to infer changes in the oxygenation of the atmosphere and the deep ocean, respectively, in the aftermath of the Stelfox glaciation (Shen *et al.* 2008). Large variability (>35‰) in $\delta^{34}S_{sulphide}$ is observed from bottom to top, indicating that sulphate was not limiting (i.e. >2 mM). This implies higher rates of oxidative weathering (the major source of marine sulphate) than before the glaciation (Hurtgen *et al.* 2002). There is a dramatic shift in the Fe-speciation ratio (FeHR/FeT), however, between 140 and 160 m above the base of the lithologically homogeneous black shale sequence that is 420 m thick in total. The average value below 140 m is 0.43 ($n = 32$), indicating bottom water anoxia, whereas above 160 m it is 0.11 ($n = 27$), which is consistent with oxygenated bottom waters (Raiswell & Canfield 1998; Lyons & Severmann 2006; Canfield *et al.* 2007).

Calcium isotopes

Calcium isotopes ($\delta^{44}Ca$) were measured in limestone of the lower Twitya Fm., and in dolostone and limestone of the Ravensthroat and Hayhook formations, respectively (Silva-Tamayo *et al.* 2010). The data from the first are consistent with mid-Cryogenian post-glacial carbonates in Brazil, and the latter with basal Ediacaran post-glacial sequences in Brazil and Namibia (Silva-Tamayo *et al.* 2010). Compared with the younger sequences, the older $\delta^{44}Ca$ profiles appear basally truncated, similar to their sequence stratigraphies and $\delta^{13}C$ profiles (Hoffman & Schrag 2002). The

younger sequences exhibit paired negative and positive $\delta^{44}Ca$ excursions that span twice the entire Phanerozoic range of variability (Farkas *et al.* 2007). The paired anomaly in the lower Hayhook limestone is preceeded (Ravensthroat Fm.) and followed (upper Hayhook Fm.) by relatively stable values lying well within the Phanerozoic range (Silva-Tamayo *et al.* 2010).

Equilibrium isotope fractionation during carbonate precipitation maintains seawater roughly 1.0‰ heavier than the sources and sinks of Ca in the ocean. Thus, imbalance between Ca input and output will cause deviations in the $\delta^{44}Ca$ of seawater, and therefore in marine carbonate. The magnitude of the equilibrium fractionation is expected to vary with temperature and carbonate precipitation rate, but relatively modest variability in $\delta^{44}Ca$ ($n = 10$) within the Ravensthroat Fm. (Silva-Tamayo *et al.* 2010), deposited during global deglaciation when changes in temperature and precipitation rate may have been large, implies that those dependencies were either small or counteracting at that time. The paired negative and positive excursions of 1.0‰ apiece in the lower Hayhook limestone and correlatives ($n = 31$) represents first, a large excess of Ca input over output, followed by the reverse, a large excess of Ca output over input (Silva-Tamayo *et al.* 2010).

Synglacial hematite jaspilite (Fe-formation), Rapitan Group

REE geochemistry of the Sayunei jaspilite (Klein & Buekes, 1993) is described in Hoffman *et al.* (2011). Planavsky *et al.* (2010) present elemental data (P, Fe, Mn and Al) for jaspilite samples from the Sayunei Fm. ($n = 41$) and correlative strata (Upper Tindir Group) in the Tatonduk inlier. In common with other Cryogenian glaciogenic jaspilites, the samples have much higher phosphate contents (average $P/Fe = 1.44\%$, $n = 44$) than Palaeoproterozoic or Archaean Fe-formations (Planavsky *et al.* 2010).

Iron isotopes ($\delta^{57}Fe$) and accompanying rare-earth elements (REE), including redox-sensitive cerium anomalies (Ce/Ce*), have been measured through the 16.4-m-thick interval of hematitic mudstone and hematite-jaspilite (banded Fe-formation) at the top of the Sayunei Fm. in the Hayhook Lake area (Fig. 36.7). The $\delta^{57}Fe$ values increase systematically upsection from −0.7‰ to 1.2‰. The largest rise coincides with the transition from hematitic mudstone to hematite-jaspilite, which also corresponds to the highest Fe concentration (*c.* 58 wt% Fe_2O_3). The increase in $\delta^{57}Fe$ is accompanied by a rise in Ce/Ce* (Fig. 36.7).

Palaeontology

Neoproterozoic palaeontology of the Mackenzie Mountains is summarized in Narbonne & Aitken (1995). When combined with contemporary work in the Wernecke Mountains (Narbonne & Hofmann 1987) and ongoing stratigraphic and palaeontological studies in correlative strata of the Tatonduk inlier, a pattern of change over time emerges that is broadly consistent with other areas (Macdonald *et al.* 2010*a*, *b*; Macdonald & Cohen 2011). A number of eukaryotic crown groups, both algal and protistan, had evolved and diversified before the Rapitan glaciation. The record of these groups is cryptic from shortly before the Rapitan glaciation until long after the Stelfox glaciation.

Soft-bodied, Ediacara-type macrofossils, representing benthic polypoid and frond-like organisms, occur in the upper Ediacaran Blueflower Fm. (Fig. 36.1), where they coexist with infaunal burrows (simple, meandering and subordinate patterned) that extend into the overlying Risky Fm. (Narbonne & Aitken 1990; Narbonne 1994). In the same area, near Sekwi Brook (Fig. 36.1), simple radially symmetric body fossils and rare trace fossils occur in the middle Sheepbed Fm. (Narbonne & Aitken 1990; Narbonne 1994). The Stelfox glaciation is not recognized at Sekwi Brook, but at Shale Lake (Fig. 36.1), Fe-speciation data indicate that bottom waters became oxygenated just below the middle Sheepbed Fm. (Shen *et al.* 2008).

An assemblage of simple, centimetric annuli and discs, thought to be biogenic, occur in the upper Twitya Fm. (Fig. 36.3a) of the Sayunei Range (Hofmann *et al.* 1990), south of Twitya River (Fig. 36.1). As possible sponge-grade metazoan fossils pre-dating the terminal Cryogenian glaciation, the 'Twitya-discs' have recently been joined by calcareous structures at different horizons

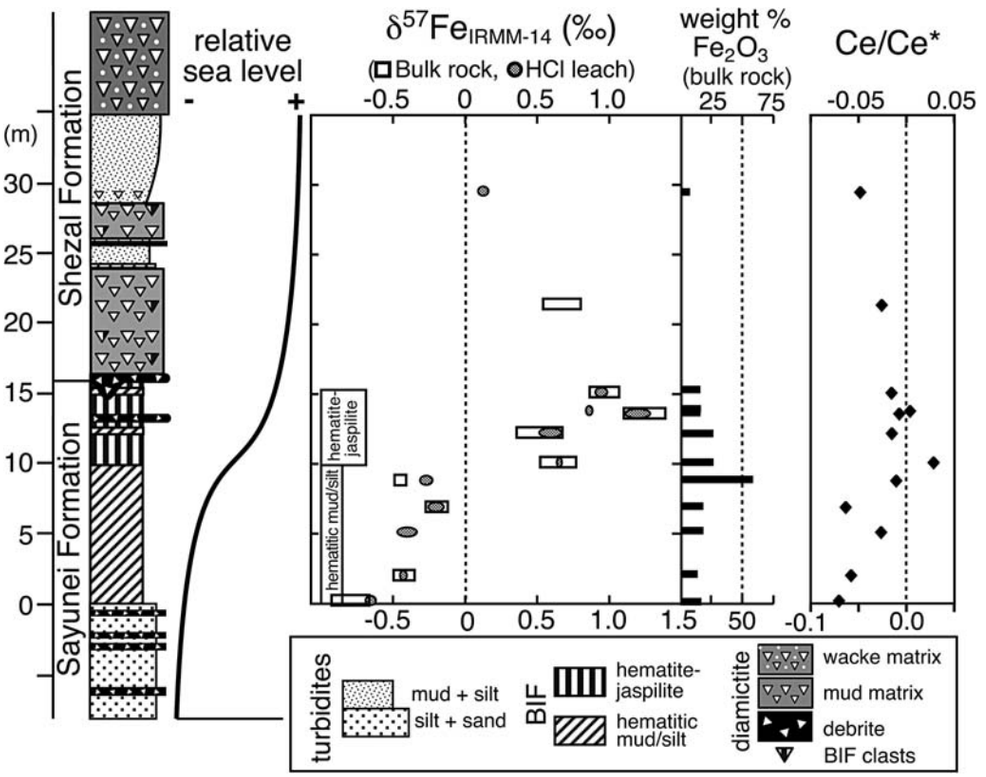

Fig. 36.7. Fe isotopes ($\delta^{57}Fe$), wt% Fe_2O_3 and Ce anomaly data (Ce/Ce*) from the Sayunei Fe-formation in the Hayhook Lake reference section. Data tabulated in Halverson *et al.* (2011).

in South Australia (Wallace & Woon 2008; Maloof *et al.* 2010), and a sponge biomarker in the Oman Salt Basin (Love *et al.* 2009).

Other characteristics

The Crest deposit at Iron Creek (Fig. 36.3d), near Snake River, is a hematite–jaspilite interval $\leq$120 m thick within glaciogenic diamictites of the Rapitan Group (Yeo 1986; Klein & Beukes 1993). The deposit contains 5.6 billion tonnes of 'ore' averaging 47.2% Fe and regional reserves are estimated to exceed 18.6 billion tonnes (Yeo 1986). Because of remoteness and difficult terrain, the deposit has never been economic.

Palaeolatitude and palaeogeography

Palaeomagnetic data from the Mackenzie Mountains relating to the Rapitan and Stelfox glaciations have been reviewed (Evans 2000; Evans & Raub 2011). Morris (1977) recognized three natural remanent magnetic components in the Rapitan Group, of which the one inferred to be the youngest (Cretaceous?) gives a high palaeolatitude and the other two give low palaeolatitudes. A larger data set obtained by Park (1997) gives broadly similar results, but only after anomalous declinations are corrected for large vertical-axis rotations of presumed structural origin. The high-inclination poles were acquired during tectonic folding and the low-inclination poles before that time, although Morris (1977) and Park (1997) disagreed on which of the two clusters of low-inclination poles was older. The palaeolatitudes of their inferred oldest components are $08 \pm 2^\circ$ (Morris 1977) and $06 \pm 7^\circ$ (Park 1997). Neither result is definitively syndepositional, but the near-equatorial palaeolatitudes agree with more recent palaeomagnetic results from mid-Neoproterozoic (800–740 Ma) sedimentary rocks in western Laurentia (Weil *et al.* 2004, 2006).

Shallow mafic igneous rocks provide more reliable palaeomagnetic results than sedimentary rocks because they are strongly magnetized, resist low-temperature remagnetization, have not been compacted (no flattening of palaeomagnetic inclination), and provide baked-contact tests of the primary age of remanent magnetization, which can be directly dated as the crystallization age of the rock. The Franklin Large Igneous Province (LIP) comprises comagmatic mafic dykes, sills and lavas extending collectively for 2500 km across Arctic Laurentia. The grand mean palaeopole (8.4°N, 163.8°E, $A_{95} = 2.8^\circ$, $n = 78$ sites) for the Franklin LIP (Denyszyn *et al.* 2009) places the Mount Harper area and the Mackenzie Mountains, respectively, at 21 ± 3 and 18 ± 3°N palaeolatitude at the time of magmatism, which spanned the onset of the Rapitan glaciation (see below). These results for the Rapitan glaciation are more reliable than those from the Rapitan Group itself.

There are no direct palaeomagnetic constraints on the Stelfox glaciation. McMechan (2000*b*) cites Park (1994) as giving a palaeolatitude of *c.* 35° for the Stelfox glaciation, but this was based on palaeopoles from the Risky Fm., which is *c.* 2 km stratigraphically above the Stelfox Member (Fig. 36.3a). Park (1994) estimated the Risky Fm. to be younger than the 615 Ma Long Range Dykes of Newfoundland and Labrador (Kamo *et al.* 1989; Kamo & Gower 1994). Although more results are needed for better statistics, the preliminary palaeopole for the Long Range Dykes (19.0°N, 355.3°E, $A_{95} = 17.4^\circ$, $n = 5$ dykes) places the Mackenzie Mountains near the palaeoequator at 615 Ma (McCausland *et al.* 2007).

Geochronological constraints

In the Mount Harper area of the Ogilvie Mountains, 310 km west of Corn Creek (Fig. 36.1), up to 120 m of massive and bedded diamictite, correlative with the lower Rapitan Group, was deposited during the waning stages of bimodal volcanism in an active rift basin (Mustard & Roots 1997; Macdonald *et al.* 2010*b*). The presence of faceted and striated clasts, bed-penetrating dropstones, common outsized and exotic clasts, and glacial push structures (Hart River inlier) within a marine succession support a glacial marine origin for the diamictite at an ice-sheet grounding-line. A quartz-phyric rhyolite within the volcanic pile, stratigraphically beneath the diamictite, and a felsic tuff within diamictite, *c.* 60 m above the base of the glacial–periglacial sequence, give U–Pb zircon dates of 717.43 ± 0.14 and 716.47 ± 0.24 Ma (2σ), respectively (Macdonald *et al.* 2010*b*). These dates are indistinguishable in age from mafic dykes and sills of the Franklin Large Igneous Province (Heaman *et al.* 1992; Denyszyn *et al.* 2009; Macdonald *et al.* 2010*b*), which straddled the palaeoequator at the time of their emplacement. The beginning of glacial marine sedimentation in the Mount Harper rift basin at 717 Ma is the best indicator of the onset of Rapitan glaciation in the northern Canadian Cordillera (Macdonald *et al.* 2010*b*). These data are consistent with maximum age constraints obtained from the Mackenzie Mountains and Windermere Supergroup, including a weighted mean $^{207}Pb/^{206}Pb$ date of 779 ± 2.3 Ma (Harlan *et al.* 2003) obtained for two baddeleyite analyses from a gabbro sill (Carcajou Canyon Gabbro) intruding the Tsezotene Fm. (Fig. 36.3), and a weighted average $^{207}Pb/^{206}Pb$ date of 755 ± 18 Ma obtained for two concordant but low-Pb zircon grains from a single leucogranite 'dropstone' within turbidites close to the base of the Sayunei Fm. near Shale Lake (Ross & Villeneuve 1997).

The Stelfox glaciation has no independent radiometric age constraint. Mafic tuffs in the upper Keele Fm. (Fig. 36.3a) contain only xenocrystic zircons. The Stelfox glaciation is assumed, largely on the basis of its post-glacial carbonate sequence, to be correlative with the terminal Cryogenian glaciation (Knoll *et al.* 2006), which terminated in 635 Ma.

Discussion

Palaeoenvironmental interpretation of the Rapitan Group

The Rapitan Group is widely interpreted as a glacial marine succession because of the occurrence of faceted and striated clasts, sand aggregates ('till pellets'), erratic dropstones with impact-related structures, and soft-sediment deformation horizons (e.g. push structures, scaly matrix in particular diamictite sheets) of apparent glacitectonic origin (Young 1976; Eisbacher 1981*a*, 1985; Yeo 1981; Aitken 1982; Macdonald *et al.* 2010*b*). Eisbacher (1985) presents a comprehensive facies model ranging from fluctuating grounding-line diamictites (Shezal Fm.) through transitional facies to distal proglacial turbidites and fine-grained suspension fallout accumulated in structurally controlled, deep-water basins (Sayunei Fm.). The distal nature of the Sayunei turbidites, characterized by Bouma C-D sequences, is emphasized (Yeo 1981; Eisbacher 1985) and the source of suspended sediment is inferred to be turbid meltwater plumes emanating from discharge sites at ice grounding-lines at the basin margin (Young 1976; Yeo 1981; Klein & Beukes 1993). Eisbacher (1985, p. 242, fig. 8) suggests that the paucity of dropstones and diamictite, respectively, in the Sayunei Fm. reflect a suppression of icebergs and a buttressing of ice grounding-lines by a 'stable sea-ice cover' (Dowdeswell *et al.* 2000). Such a permanent ice cover would account for the low organic content and deep maroon colour of the Sayunei mudrocks, in contrast to the basinal shale and limestone of the underlying non-glacial Copper Cap Fm., which are mostly fetid and black in colour. Removal of the permanent ice cover by climate warming would have allowed icebergs and ice grounding-lines to advance basinward at the time of the Sayunei-Shezal transition (Eisbacher 1985).

Palaeomagnetic data place the Rapitan rift basins in palaeolatitudes comparable to the present southern Red Sea Rift basin (Evans & Raub 2011). At the Last Glacial Maximum (LGM, *c.* 20 ka), arguably as severe a glaciation as any in the Phanerozoic eon, the lowest nearby glacial moraines, in the Ethiopian Highlands, are 3750 m above sea level (Umer *et al.* 2004). Air temperatures at that altitude are on average 26 °C colder than the same latitude at sea level, reached by Rapitan glaciers. This gives some sense of the contrast between the Rapitan glaciation and the LGM.

Origin of 'transitional-facies' Fe-formation

A local hydrothermal source of Fe for transitional-facies Fe-formation (Fig. 36.3d) was favoured by Yeo (1981) and Young (1988, 2002). However, when compared with Neoarchaean and Palaeoproterozoic Fe-formations, the rare-earth element (REE) chemistry of the Rapitan Fe-formation is 'much less distinctly influenced by hydrothermal input', suggesting that such input was 'highly diluted by ocean waters at Rapitan time' (Klein & Beukes 1993). Moreover, where submarine volcanism was demonstratively active during the Rapitan glaciation (Mount Harper area), Fe-formation is absent. Where Fe-formation is present, in the Tatonduk inlier (Macdonald & Cohen 2011) and the Mackenzie Mountains, interbedded volcanic rocks are non-existent (Macdonald *et al.* 2010*b*).

Global Fe-speciation data suggest that Cryogenian and Ediacaran deep waters were ferruginous, rather than euxinic (Canfield *et al.* 2008). This raises the question why Fe-formation (hematite jaspilite) was only deposited during glacial times, and possibly only during the 'Sturtian' glaciation (Hoffman *et al.* 2011). If the Rapitan rift-basins were covered by thick permanent marine ice during fine-grained sedimentation of the Sayunei Fm. (Eisbacher 1985), primary productivity would have crashed, limiting bacterial sulphate reduction and allowing high concentrations of Fe in acidic waters in the absence of hydrothermal sources (Mikucki *et al.* 2009). The Crest Fe deposit at Iron Creek (Fig. 36.3d) is situated within a sequence of transitional-facies diamictites (Eisbacher 1985), where local oxidizing power capable of titrating dissolved Fe would have been provided by subglacial meltwater discharges at basin-margin ice grounding-lines, assuming air bubbles in the meteoric ice (compressed snow) contained oxygen.

Low primary productivity related to the permanent ice cover as well as low seawater pH would account for elevated P/Fe ratios in the Fe-formation at Iron Creek and perhaps other synglacial Cryogenian Fe-formations (Planavsky *et al.* 2010). The explanation for the high P/Fe ratio favoured by Planavsky *et al.* (2010) involves 'unprecedented continental P fluxes during postglacial and interglacial time periods, given the extraordinary extent and duration of Cryogenian ice cover and the high levels of P delivery expected from glaciated catchments'. The problem with their explanation is that six of the seven Cryogenian Fe-formations in their database were deposited *before* the termination of the first major Cryogenian glaciation.

Origin and stratigraphic localization of 'basin-facies' Fe-formation

Why does Fe-formation in the basin facies (Eisbacher 1985) occur at the top of the Sayunei Fm., disconformably beneath the Shezal diamictite (Fig. 36.3b,c)? If we accept Eisbacher's (1985) explanation that the advance of the Shezal grounding-line was triggered by the removal of permanent sea ice over the basin, two factors would have contributed to the deposition of Fe-formation. First, as the ice cover thinned and finally disappeared, anoxic and oxygenic photosynthesis could have precipitated Fe_2O_3-precursor from anoxic Fe(II)-rich basin waters. Second, after the ice cover was removed, air–sea gas exchange and wind-driven mixing would have quickly oxygenated the surface waters, leading to abiotic Fe(III) precipitation.

After the Sayunei basin became ice-free, the water vapour content of air blowing across the basin would have increased due to evaporation. This would likely have caused a positive change in the mass-balance of downwind ice sheets, due to increased precipitation and decreased melting on account of fog and clouds. On a 'modern Snowball Earth' (i.e. present geography with complete sea-ice cover, Voigt & Marotzke 2009), the Red Sea Rift would be isolated from the Indian Ocean because of the roughly 1.0 km fall in global mean sea level (glacioeustasy). As tropical sea-surface temperatures rose to melting point, sea ice on the Red Sea basin would disappear, while the Indian Ocean would remain ice-bound because of sea–glacial flow from the south (Warren *et al.* 2002; Goodman & Pierrehumbert 2003). Accordingly, the Shezal diamictite would represent the time interval between the opening of the Sayunei basin 'oasis' and overall glacial termination. Once illuminated, primary productivity in the basin, now crowded with icebergs, would be stimulated.

Fe-isotope and Ce-anomaly data (Fig. 36.7) shed additional light on the basin-facies Fe-formation near Hayhook Lake (Fig. 36.3c). Controls on Fe-isotope variation in natural systems are not well known, and data from ancient rocks are still quite limited. Laboratory experiments indicate that broadly similar equilibrium and kinetic isotope fractionations are associated with both abiotic and biological Fe-oxidation pathways (Johnson & Beard 2006). Consider the $\delta^{57}Fe$ trend in the Fe-formation (Fig. 36.7) not in terms of a secular change in seawater Fe-isotope composition, but as a change in net Fe-isotope fractionation ($\Delta^{57}Fe_{hem\text{-}Fe2+}$) between hematite (or ferric-oxyhydroxide precursor) and dissolved Fe(II) across a redox chemocline in the water column (Halverson *et al.* 2011). This could come about either because the Fe-isotope fractionation varied as a function of the Fe(II) concentration, assumed to increase with depth across the chemocline, or because of progressive oxidation of Fe(II) as it upwelled across the chemocline. Progressive oxidation would drive the isotopic composition of the dissolved Fe(II) to more ^{57}Fe-depleted values, lowering the $\delta^{57}Fe$ of the hematite produced. In either case, the $\delta^{57}Fe$ of hematite should decrease from the base of the chemocline to the top. Accordingly, the upward increase in $\delta^{57}Fe$ observed within the Fe-formation (Fig. 36.7) suggests an increase in water depth with time, which is consistent with more reducing conditions up-section inferred from the Ce/Ce* data and with transgression inferred on sedimentological grounds over the same stratigraphic interval (Klein & Beukes 1993). As the Sayunei Fe-formation is directly overlain by the Shezal diamictite (Fig. 36.3), the rise in relative sea level is logically attributed to lithospheric downwarping under the load of the advancing Shezal ice sheet (Halverson *et al.* 2011).

Palaeoenvironmental interpretation of the Stelfox (Ice Brook) glaciation

The Stelfox Member of the Ice Brook Fm. is a subaqueous unit interpreted as glaciomarine because of the presence of faceted and striated clasts in diamictite, sand and granule aggregates ('till pellets'), dropstones with impact-related structures in finely laminated mudrocks, extremely angular quartz grains derived from well-rounded quartz arenites of the Keele Fm., and diamictite in a shallow-shelf setting where large-scale mass-flows are less likely to occur (Aitken 1991*a*, *b*).

In discussing the Stelfox-equivalent Vreeland Diamictites in northeastern British Columbia, McMechan (2000*a*, *b*) described mud-rich diamictites and related fine-grained terrigenous facies as resembling deposits associated with temperate, wet-based glaciers in southern Alaska, in contrast to those of cold-based glaciers in Antarctica. She argued that they are inconsistent with the existence of a Cryogenian 'Snowball' Earth, assuming that its

mean-annual tropical surface temperature was close to that of present-day Antarctica. She noted the prevalence of biogenic facies (e.g. diatomaceous ooze) beneath Antarctic ice shelves, on the Antarctic continental shelf and adjacent to the outlets of fast-flowing ice streams, implying a near-absence of fine-grained terrigenous input from meltwater plumes (Domack 1988; Anderson *et al.* 1991). Citing the same authors, she posited that significant meltwater flow requires surface melting and therefore summer air temperatures above 0 °C, which do not occur on Antarctica or on a 'Snowball' Earth (McMechan 2000*b*).

Much has been learned about the Antarctic glacial regime since the studies cited by McMechan (2000*a*, *b*). More than 150 subglacial lakes have been found, some at the origins of fast-flowing ice streams, and they are not stagnant but are subject to active hydrodynamic exchange (Siegert *et al.* 2005; Wingham *et al.* 2006; Bell *et al.* 2007). Modelling suggests that basal melting occurs under most of the interior of the East Antarctic Ice Sheet and all of its outlet ice streams (Pattyn 2010). Recent collapse of the Larsen B ice shelf revealed the former existence of both terrigenous and biogenic sedimentation beneath the ice shelf (Domack *et al.* 2005; Damiani & Giorgetti 2008). Springtime diatom blooms on the East Antarctic margin may be triggered, not inhibited, by Fe-rich sub-glacial meltwater disharges, from which terrigenous mud subsequently settles (Leventer *et al.* 2006). There is no doubt that accumulation rates for muds are lower in polar than in temperate settings, but sedimentation rates in the Cryogenian are as yet unknown in the absence of biogenic facies, varve chronologies, or data on meteoritic dust content. We agree that 'any model for Neoproterozoic glaciation should include a significant period of more moderate glacial conditions prior to the end of glaciation' (McMechan 2000*b*), but we maintain that even the most extreme glaciation must experience more moderate conditions at its termination, especially in tropical marine environments, and that this is fully consistent with the hysteresis loop predicted by the Snowball Earth hypothesis (Hoffman 2009).

Calcium isotope record of the Stelfox glaciation and its aftermath

The Snowball Earth hypothesis (Hoffman & Schrag 2002) provides a potential explanation for the paired negative and positive δ^{44}Ca excursions and for their stratigraphic location in the lower Hayhook Fm. (Silva-Tamayo *et al.* 2010). During a snowball glaciation, a steady rise in CO_2 drives carbonate dissolution in the ocean (a source of Ca) and precludes carbonate deposition (Hoffman & Schrag 2002, fig. 10). This is consistent with the absence of primary carbonate in the relevant synglacial strata. The δ^{44}Ca of dissolved Ca in snowball brine should therefore fall towards the value of the Ca input. The first carbonate that precipitates from the brine will be depleted in ^{44}Ca by *c.* 1.0‰ compared with normal carbonates. In the snowball aftermath, Ca input to the ocean from erosion is high, but rapid ocean warming and the more leisurely drawdown of CO_2, through silicate weathering, drive excess Ca output (carbonate deposition) over input, raising δ^{44}Ca. During deglaciation, however, ocean surface waters are flooded by glacial meltwater, marine and terrestrial, and are thus isolated from the deep brine by an exceptionally stable density stratification (Shields 2005). Consequently, the ^{44}Ca-depleted snowball signature is not observed in the Ravensthroat Fm., which was deposited in surface waters during the snowball meltdown (James *et al.* 2001). As melting neared completion, the flux of meltwater waned and ocean mixing by winds and tides resumed. The negative δ^{44}Ca excursion in the lower Hayhook Fm. (Silva-Tamayo *et al.* 2010) records the mixing of ^{44}Ca-depleted snowball brine and the meltwater lid. It does not record the generation of the isotope anomaly in dissolved Ca of the brine, but rather its delayed expression as precipitated carbonate when the brine was mixed into the meltwater lid, which was saturated with carbonate from dissolution of carbonate rock 'flour', exposed by deglaciation (Fairchild 1993). Once the ocean was mixed, the post-glacial excess of Ca output over input drove the positive δ^{44}Ca excursion. Silva-Tamayo *et al.* (2010), who assume that the stratigraphic expression of the negative δ^{44}Ca excursion corresponds to its time of formation, attribute the negative excursion to Ca influx from weathering immediately after deglaciation. Their model requires that Ca input greatly exceeded output, which appears unlikely at a time of ocean warming (raising saturation) and mixing (facilitating degassing), when the surface ocean is known to have been critically oversaturated from the widespread occurrence of syndeglacial cap dolostones (Hoffman *et al.* 2007).

Correlation and palaeogeography

The post-glacial carbonate sequences following the older and younger Cryogenian glaciations are stratigraphically, lithologically and isotopically distinct (Kennedy *et al.* 1998; Hoffman & Schrag 2002). They provide a surprisingly successful basis for distinguishing the glaciations globally (Knoll *et al.* 2006; Hoffman *et al.* 2011). As cosmopolitans, however, they are less well suited for palaeogeographic reconstruction. In a wide orogen like the North American Cordillera, the distinction between Neoproterozoic successions that are indigenous to Laurentia and those originating elsewhere is fundamental (Johnston 2008; Hildebrand 2009). All exposed Neoproterozoic rocks in the Mackenzie Mountains (Fig. 36.1) were thrust northeastward relative to cratonic Laurentia in the Upper Cretaceous–Paleocene. Sequence and chemostratigraphic comparison of successions deposited before, between and after the Cryogenian glaciations implies that the Tatonduk, Coal Creek, Hart River and Wernecke inliers of the Yukon Territory expose a Neoproterozoic succession continuous with that of the Mackenzie Mountains (Macdonald & Roots 2009; Macdonald *et al.* 2010*a*, *b*; Macdonald & Cohen 2011). The co-occurrence of 718–716 Ma mafic magmatism in the Mount Harper area (Coal Creek inlier) and on cratonic Laurentia (Franklin LIP) therefore implies that the Neoproterozoic succession of the Ogilvie and Mackenzie Mountains formed on the margin of Laurentia.

In contrast, the lithostratigraphically alien Katakturuk Dolomite (Ediacaran) in the northeastern Brooks Range, Arctic Alaska, is unlikely to have had a Laurentian affinity before Siluro-Devonian time, at the earliest (Macdonald *et al.* 2009). Accordingly, the stratigraphically underlying Hula Hula diamictite represents a Cryogenian glaciation of Chukotka-Arctic Alaska, not Laurentia, and the Mount Copleston volcanics within and beneath the diamictite are predicted to be asynchronous with the Franklin LIP.

What about Neoproterozoic successions in the rest of the North American Cordillera? They host named glacial horizons in British Columbia (Toby and Vreeland), Idaho (Scout Mountain), Utah (Dutch Peak and Mineral Fork), California (Surprise and Wildrose) and Sonora (Mina el Mezquite). Conventionally, all have been assumed to originate at the rifted margin of Laurentia (Stewart 1972). In the Cordilleran collisional model (Johnston 2008; Hildebrand 2009), all except possibly the Mineral Fork originated elsewhere. In that model, they collided with the Laurentian margin in the Late Cretaceous as part of a composite ribbon continent named 'Rubia' (Hildebrand 2009) or 'Saybia' (Johnston 2008). Targeted detrital zircon dating of the various glacial horizons, and their host successions, should be an effective means of testing the Rubia/Saybia hypothesis. From the perspective of the Mackenzie Mountains, the sequence stratigraphy and lithology of Neoproterozoic successions assigned to the Windermere Supergroup in British Columbia (Ross *et al.* 1989) and to the South are not similar. The differences may reflect facies changes, as conventionally assumed, but it seems fair to conclude that Neoproterozoic strata of the North American Cordillera provide no grounds at present for rejecting the Rubia/Saybia hypothesis. To date, all

that we do know is that palaeomagnetic data from the Franklin LIP place the then northward-facing rifted margin of Laurentia in the Mackenzie Mountains at $18 \pm 3^{\circ}$N latitude at the onset of the Rapitan glaciation, and possibly closer to the palaeo-equator during the Stelfox glaciation.

Fieldwork in the Mackenzie Mountains was licensed by the Aurora Research Institute and supported by a grant from the Astrobiology Institute of the US National Aeronautics and Space Administration (NASA), and by grants EAR-9905495 and EAR-0417422 from the US National Science Foundation (NSF) to P.F.H. C. A. Ferguson, M. T. Hurtgen, F. A. Macdonald, A. C. Maloof, Y. Shen and A. V. Turchyn participated in the fieldwork. C and O isotopes were analysed at the Laboratory for Geochemical Oceanography at Harvard University, directed by D. P. Schrag. Sr isotope data were obtained at the Geochronology Laboratory at the Massachusetts Institute of Technology, directed by S. A. Bowring. Fe isotopes were measured at the Laboratoire des Mécanismes et Transferts en Géologie (LMTG) at the Université P. Sabatier, Toulouse, France, directed by F. Poitrasson. P.F.H. acknowledges discussions with J. D. Aitken, R. W. Dalrymple, E. W. Domack, G. H. Eisbacher, H. Gabrielse, L. M. Heaman, H. J. Hofmann, N. P. James, C. W. Jefferson, A. J. Kaufman, T. Kurt Kyser, M. E. McMechan, W. A. Morris, D. C. Murphy, G. M. Narbonne, J. K. Park, G. M. Ross, G. M. Yeo and G. M. Young. Comments by E. Arnaud, G. Narbonne, E. C. Turner and G. Yeo substantially improved the manuscript. This represents a contribution of the IUGS- and UNESCO-funded IGCP (International Geoscience Programme) project #512.

References

Aitken, J. D. 1981. Stratigraphy and sedimentology of the Upper Proterozoic Little Dal Group, Mackenzie Mountains, Northwest Territories. *In*: Campbell, F. H. A. (ed.) *Proterozoic Basins of Canada*. Geological Survey of Canada Paper, **81–10**, 47–71.

Aitken, J. D. 1982. Precambrian of the Mackenzie fold belt — a stratigraphic and tectonic overview. *In*: Hutchinson, R. W., Spence, C. D. & Franklin, J. M. (eds) *Precambrian Sulfide Deposits*. Geological Association of Canada Special Paper, **25**, 149–161.

Aitken, J. D. 1991*a*. Two late Proterozoic glaciations, Mackenzie Mountains, northwestern Canada. *Geology*, **19**, 445–448.

Aitken, J. D. 1991*b*. The Ice Brook Formation and post-Raptian, Late Proterozoic glaciation, Mackenzie Mountains, Northwest Territories. *Geological Survey of Canada Bulletin*, **404**.

Aitken, J. D. & Long, D. G. F. 1978. Mackenzie tectonic arc – reflection of early basin configuration? *Geology*, **6**, 626–629.

Allen, P. A. & Hoffman, P. F. 2005. Extreme winds and waves in the aftermath of a Neoproterozoic glaciation. *Nature*, **433**, 123–127.

Anderson, J. B., Kennedy, D. S., Smith, M. J. & Domack, E. W. 1991. Sedimentary facies associated with Antarctica's floating ice masses. *In*: Anderson, J. B. & Ashley, G. M. (eds) *Glacial Marine Sedimentation: Paleoclimatic Significance*. Geological Society of America Special Paper, **261**, 1–25.

Assereto, R. L. A. M. & Kendall, C. G. St. C. 1977. Nature, origin and classification of peritidal tepee structures and related breccas. *Sedimentology*, **24**, 153–210.

Bell, R. E., Studinger, M., Shuman, C. A., Fahnestock, M. A. & Joughin, I. 2007. Large subglacial lakes in East Antarctica at the onset of fast-flowing ice streams. *Nature*, **445**, 904–907.

Canfield, D. E., Poulton, S. W. & Narbonne, G. M. 2007. Late-Neoproterozoic deep-ocean oxygenation and the rise of animal life. *Science*, **315**, 92–95.

Canfield, D. E., Poulton, S. W., Knoll, A. H., Narbonne, G. M., Ross, G., Goldberg, T. & Strauss, H. 2008. Ferruginous conditions dominated later Neoproterozoic deep-water chemistry. *Science*, **321**, 949–952.

Dalrymple, R. W. & Narbonne, G. M. 1996. Continental slope sedimentation in the Sheepbed Formation (Neoproterozoic, Windermere Supergroup), Mackenzie Mountains, N.W.T. *Canadian Journal of Earth Sciences*, **33**, 848–862.

Damiani, D. & Giorgetti, G. 2008. Provenance of glacial-marine sediments under the McMurdo/Ross Ice Shelf (Windless Bight, Antarctica): Heavy minerals and geochemical data. *Palaeogeography, Palaeoclimatology, Palaeoecology*, **260**, 262–283.

Day, E. S., James, N. P., Narbonne, G. M. & Dalrymple, R. W. 2004. A sedimentary prelude to Marinoan glaciation, Cryogenian (Middle Neoproterozoic) Keele Formation, Mackenzie Mountains, northwestern Canada. *Precambrian Research*, **133**, 223–247.

Denyszyn, S. W., Halls, H. C., Davis, D. W. & Evans, D. A. D. 2009. Paleomagnetism and U–Pb geochronology of Franklin dykes in High Arctic Canada and Greenland: a revised age and paleomagnetic pole constraining block rotations in the Nares Strait region. *Canadian Journal of Earth Sciences*, **46**, 689–705.

Domack, E. W. 1988. Biogenic facies in the Antarctic glacimarine environment: basis for a polar glacimarine summary. *Palaeogeography, Palaeoclimatology, Palaeoecology*, **63**, 357–372.

Domack, E. W., Duran, D. *et al*. 2005. Stability of the Larsen B ice shelf on the Antarctic Peninsula during the Holocene epoch. *Nature*, **436**, 681–685.

Dowdeswell, J. A., Whittington, J. A., Jennings, A. E., Andrews, J. T., Mackensen, A. & Marienfield, P. 2000. An origin for laminated glacimarine sediments through sea-ice build-up and suppressed iceberg rafting. *Sedimentology*, **47**, 557–576.

Eisbacher, G. H. 1978. *Re-definition and Subdivision of the Rapitan Group, Mackenzie Mountains*. Geological Survey of Canada Paper **77–35**.

Eisbacher, G. H. 1981*a*. Sedimentary tectonics and glacial record in the Windermere Supergroup, Mackenzie Mountains, northwestern Canada. *Geological Survey of Canada Paper*, **80–27**.

Eisbacher, G. H. 1981*b*. Late Precambrian tillites of the northern Yukon-Northwest Territories region, Canada. *In*: Hambrey, M. J. & Harland, W. B. (eds) *Earth's Pre-Pleistocene Glacial Record*. Cambridge University Press, Cambridge, 724–727.

Eisbacher, G. H. 1985. Late Proterozoic rifting, glacial sedimentation and sedimentary cycles in the light of Windermere deposition, western Canada. *Palaeogeography, Palaeoclimatology, Palaeoecology*, **51**, 231–254.

Evans, D. A. D. 2000. Stratigraphic, geochronological and Paleomagnetic constraints upon the Neoproterozoic climatic paradox. *American Journal of Science*, **300**, 347–433.

Evans, D. A. D. & Raub, T. D. 2011. Neoproterozoic glacial Palaeolatitudes: a global update. *In*: Arnaud, E., Halverson, G. P. & Shields, G. (eds) *The Geological Record of Neoproterozoic Glaciations*. Geological Society, London, Memoirs, **36**, 93–112.

Fairchild, I. J. 1993. Balmy shores and ice wastes: the paradox of carbonates associated with glacial deposits in Neoproterozoic times. *Sedimentology Review*, **1**, 1–16.

Farkas, J., Böhm, F. *et al*. 2007. Calcium isotope record of Phanerozoic oceans: implications for chemical evolution of seawater and its causative mechanisms. *Geochimica et Cosmochimica Acta*, **71**, 5117–5134.

Friedman, I. & O'Neil, J. R. 1977. Chapter KK. Compilation of stable isotope fractionation factors of geochemical interest. *In*: Fleischer, M. (ed.) *Data of Geochemistry* 6th edn. United States Geological Survey Professional Paper **440–KK**, Washington, DC.

Gabrielse, H., Blusson, S. L. & Roddick, J. A. 1973. *Geology of the Flat River, Glacier Lake and Wrigley Lake map-areas, District of Mackenzie and Yukon Territory*. Geological Survey of Canada Memoir **366**.

Goodman, J. & Pierrehumbert, R. T. 2003. Glacial flow of floating marine ice in 'Snowball Earth'. *Journal of Geophysical Research*, **108**, 3308, doi: 10.1029/2002JC001471.

Green, L. H. & Godwin, C. I. 1963. *Snake River area: mineral industry of Yukon Territory and southwestern District of Mackenzie, 1962*. Geological Survey of Canada Paper **63–38**, 15–18.

Halverson, G. P. 2006. A Neoproterozoic chronology. *In*: Xiao, S. & Kaufman, A. J. (eds) *Neoproterozoic Geobiology and Paleobiology*. Springer, Dordrecht, 231–271.

Halverson, G. P., Maloof, A. C. & Hoffman, P. F. 2004. The Marinoan glaciation (Neoproterozoic) in northeast Svalbard. *Basin Research*, **16**, 297–324.

Halverson, G. P., Dudás, F. Ö., Maloof, A. C. & Bowring, S. A. 2007. Evolution of the $^{87}Sr/^{86}Sr$ composition of Neoproterozoic seawater. *Palaeogeography, Palaeoclimatology, Palaeoecology*, **256**, 103–129.

Halverson, G. P., Poitrasson, F., Hoffman, P. F., Nedelec, A., Montel, J.-M. & Kirby, J. 2011. Fe isotope and trace element geochemistry of the Neoproterozoic syn-glacial Raptian iron formation. *Earth and Planetary Science Letters*, doi: 10.1016/j.epsl.2011.06.21.

Hambrey, M. J. & Spencer, A. M. 1987. *Late Precambrian Glaciation of Central East Greenland*. Meddelelser om Grønland, Geoscience **19**.

Harlan, S. S., Heaman, L., LeCheminant, A. N. & Premo, W. R. 2003. Gunbarrel mafic magmatic event: a key 780 Ma time marker for Rodinia plate reconstructions. *Geology*, **31**, 1053–1056.

Heaman, L. M., LeCheminant, A. N. & Rainbird, R. H. 1992. Nature and timing of Franklin igneous events, Canada: implications for a Late Proterozoic mantle plume and the break-up of Laurentia. *Earth and Planetary Science Letters*, **109**, 117–131.

Hildebrand, R. S. 2009. *Did westward subduction cause Cretaceous-Tertiary orogeny in the North American Cordillera?* Geological Society of America, Special Paper **457**.

Hoffman, P. F. 2009. Pan-glacial – a third state in the climate system. *Geology Today*, **25**, 107–114.

Hoffman, P. F. & Schrag, D. P. 2002. The snowball Earth hypothesis: testing the limits of global change. *Terra Nova*, **14**, 129–155.

Hoffman, P. F. & Macdonald, F. A. 2010. Sheet-crack cements and early regression in Marinoan (635 Ma) cap dolostones: regional benchmarks of vanishing ice-sheets? *Earth and Planetary Science Letters*, **300**, 374–384.

Hoffman, P. F., Halverson, G. P., Domack, E. W., Husson, J. M., Higgins, J. A. & Schrag, D. P. 2007. Are basal Ediacaran (635 Ma) post-glacial 'cap dolostones' diachronous? *Earth and Planetary Science Letters*, **258**, 114–131.

Hoffman, P. F., Macdonald, F. A. & Halverson, G. P. 2011. Chemical sediments associated with Neoproterozoic glaciation: iron formation, cap carbonate, barite and phosphorite. *In*: Arnaud, E., Halverson, G. P. & Shields, G. (eds) *The Geological Record of Neoproterozoic Glaciations*. Geological Society, London, Memoirs, **36**, 67–80.

Hofmann, H. J., Narbonne, G. M. & Aitken, J. D. 1990. Ediacaran remains from intertillite beds in northwestern Canada. *Geology*, **18**, 1199–1202.

Hurtgen, M. T., Arthur, M. A., Suits, N. S. & Kaufman, A. J. 2002. The sulfur isotopic composition of Neoproterozoic seawater sulfate: implications for a snowball Earth? *Earth and Planetary Science Letters*, **203**, 413–429.

Hurtgen, M. T., Halverson, G. P., Arthur, M. A. & Hoffman, P. F. 2006. Sulfur cycling in the aftermath of a 635-Ma snowball glaciation: evidence for a syn-glacial sulfidic deep ocean. *Earth and Planetary Science Letters*, **245**, 551–570.

James, N. P., Narbonne, G. M. & Kyser, T. K. 2001. Late Neoproterozoic cap carbonates: Mackenzie Mountains, northwestern Canada: precipitation and global glacial meltdown. *Canadian Journal of Earth Science*, **38**, 1229–1262.

James, N. P., Narbonne, G. M., Dalrymple, R. W. & Kyser, T. K. 2005. Glendonites in Neoproterozoic low-latitude, interglacial, sedimentary rocks, northwest Canada: insights into Cryogenian ocean and Precambrian cold-water carbonates. *Geology*, **33**, 9–12.

Jefferson, C. W. 1983. *The Upper Proterozoic Redstone Copper Belt, Mackenzie Mountains, Northwest Territories*. PhD thesis, University of Western Ontario, London, Ontario, 445.

Jefferson, C. W. & Ruelle, J. C. L. 1986. The Late Proterozoic Redstone Copper Belt, Mackenzie Mountains, Northwest Territories. *In*: Morin, J. A. (ed.) *Mineral Deposits of Northern Cordillera*. Canadian Institute of Mining and Metallurgy Special Volume, **37**, 154–168.

Johnson, C. M. & Beard, B. L. 2006. Fe isotopes: an emerging technique for understanding modern and ancient biogeochemical cycles. *GSA Today*, **16**, 4–10.

Johnston, S. T. 2008. The Cordilleran ribbon continent of North America. *Annual Reviews of Earth and Planetary Sciences*, **36**, 495–530.

Kamo, S. L. & Gower, C. F. 1994. Note: U–Pb baddeleyite dating clarifies age of characteristic paleomagnetic remanence of Long Range dykes, southeastern Labrador. *Atlantic Geology*, **30**, 259–262.

Kamo, S. L., Gower, C. F. & Krogh, T. E. 1989. Birthplace for the Iapetus Ocean? A precise U–Pb zircon and baddeleyite age for the Long Range dikes, southeast Labrador. *Geology*, **17**, 602–605.

Kaufman, A. J., Jacobsen, S. B. & Knoll, A. H. 1993. The Vendian record of Sr and C isotopic variations in seawater: implications for tectonics and paleoclimate. *Earth and Planetary Science Letters*, **120**, 409–430.

Kaufman, A. J., Knoll, A. H. & Narbonne, G. M. 1997. Isotopes, ice ages and terminal Proterozoic earth history. *Proceedings of the National Academy of Sciences (USA)*, **94**, 6600–6605.

Kendall, C. G. St. C. & Warren, J. 1987. A review of the origin and setting of tepees and their associated fabrics. *Sedimentology*, **34**, 1007–1027.

Kennedy, M. J. 1996. Stratigraphy, sedimentology and isotopic geochemistry of Australian Neoproterozoic postglacial cap dolostones: deglaciation, $\delta^{13}C$ excursions and carbonate precipitation. *Journal of Sedimentary Research*, **66**, 1050–1064.

Kennedy, M. J., Runnegar, B., Prave, A. R., Hoffmann, K.-H. & Arthur, M. A. 1998. Two or four Neoproterozoic glaciations? *Geology*, **26**, 1059–1063.

Klein, C. & Beukes, N. J. 1993. Sedimentology and geochemistry of the glaciogenic Late Proterozoic Rapitan Fe-formation in Canada. *Economic Geology*, **88**, 542–565.

Knoll, A. H., Walter, M. R., Narbonne, G. M. & Christie-Blick, N. 2006. The Ediacaran Period: a new addition to the geologic time scale. *Lethaia*, **39**, 13–30.

Leventer, A., Domack, E. *et al.* 2006. Marine sediment record from the East Antarctic margin reveals dynamics of ice sheet recession. *GSA Today*, **16**, 4–10.

Love, G. D., Grosjean, E. *et al.* 2009. Fossil steroids record the appearance of Demospongiae during the Cryogenian period. *Nature*, **457**, 718–721, doi: 10.1038/nature07673.

Lyons, T. W. & Severmann, S. 2006. A critical look at iron paleoredox proxies based on new insights from modern euxinic marine basins. *Geochimica et Cosmochimica Acta*, **70**, 5698–5722.

Macdonald, F. A. & Roots, C. F. 2009. Upper Fifteenmile Group in the Ogilvie Mountains and correlations of early Neoproterozoic strata in the northern Cordillera. *In*: MacFarlane, K. E., Weston, L. H. & Blackburn, L. R. (eds) *Yukon Exploration and Geology 2009*, Yukon Geological Survey, Whitehorse, 237–252.

Macdonald, F. A. & Cohen, P. A. 2011. The Tatonduk inlier, Alaska-Yukon border. *In*: Arnaud, E., Halverson, G. P. & Shields, G. (eds) *The Geological Record of Neoproterozoic Glaciations*. Geological Society, London, Memoirs, **36**, 389–396.

Macdonald, F. A., Mcclelland, W. C., Schrag, D. P. & Macdonald, W. P. 2009. Neoproterozoic glaciation on a carbonate platform margin in Arctic Alaska and the origin of the North Slope subterrane. *Geological Society of America Bulletin*, **121**, 448–473.

Macdonald, F. A., Cohen, P. A., Dudás, F. Ö. & Schrag, D. P. 2010*a*. Early Neoproterozoic siliceous scale microfossils in the Lower Tindir Group of Alaska and the Yukon Territory. *Geology*, **38**, 143–146.

Macdonald, F. A., Schmitz, M. D. *et al.* 2010*b*. Calibrating the Cryogenian. *Science*, **327**, 1241–1243.

Maloof, A. C., Rose, C. V. *et al.* 2010. Possible animal-body fossils in pre-Marinoan limestones from South Australia. *Nature Geoscience*, **3**, 653–659.

McCausland, P. J. A., Van der Voo, R. & Hall, C. M. 2007. Circum-Iapetus paleogeography of the Precambrian–Cambrian transition with a new paleomagnetic constraint from Laurentia. *Precambrian Research*, **156**, 125–152.

McMechan, M. E. 2000*a*. Vreeland Diamictites – Neoproterozoic glaciogenic slope deposits, Rocky Mountains, northeast British Columbia. *Bulletin of Canadian Petroleum Geology*, **48**, 246–261.

McMechan, M. E. 2000*b*. Reply to discussion. Vreeland Diamictites – Neoproterozoic glaciogenic slope deposits, Rocky Mountains, northeast British Columbia. *Bulletin of Canadian Petroleum Geology*, **48**, 364–366.

Mikucki, J. A., Pearson, A. *et al.* 2009. A contemporary microbially maintained subglacial ferrous 'ocean'. *Science*, **324**, 397–400.

Morris, W. A. 1977. Paleolatitude of upper Precambrian glaciogenic Rapitan Group and the use of tillites as chronostratigraphic marker horizons. *Geology*, **5**, 85–88.

Mustard, P. S. & Roots, C. F. 1997. Rift-related volcanism, sedimentation and tectonic setting of the Mount Harper Group, Ogilvie Mountains, Yukon Territory. *Geological Survey of Canada Bulletin*, **492**.

NARBONNE, G. M. 1994. New Ediacaran fossils from the Mackenzie Mountains, northwestern Canada. *Journal of Palaeontology*, **68**, 411–416.

NARBONNE, G. M. & HOFMANN, H. J. 1987. Ediacaran biota of the Wernecke Mountains, Yukon, Canada. *Palaeontology*, **30**, 647–676.

NARBONNE, G. M. & AITKEN, J. D. 1990. Ediacaran fossils from the Sekwi Brook area, Mackenzie Mountains, northwestern Canada. *Palaeontology*, **33**, 945–980.

NARBONNE, G. M. & AITKEN, J. D. 1995. Neoproterozoic of the Mackenzie Mountains, northwestern Canada. *Precambrian Research*, **73**, 101–121.

NARBONNE, G. M., KAUFMAN, A. J. & KNOLL, A. H. 1994. Integrated chemostratigraphy and biostratigraphy of the Windermere Supergroup, northwestern Canada: implications for Neoproterozoic correlations and early evolution of animals. *Geological Society of America Bulletin*, **106**, 1281–1292.

OVENSHINE, T. A. 1970. Observations of ice rafting in Glacier Bay, Alaska, and the identification of ancient ice-rafted deposits. *Geological Society of America Bulletin*, **81**, 891–894.

PARK, J. K. 1994. Palaeomagnetic constraints on the position of Laurentia from middle Neoproterozoic to Early Cambrian times. *Precambrian Research*, **69**, 95–112.

PARK, J. K. 1997. Paleomagnetic evidence for low-latitude glaciation during deposition of the Neoproterozoic Rapitan Group, Mackenzie Mountains, N.W.T., Canada. *Canadian Journal of Earth Sciences*, **34**, 34–49.

PATTYN, F. 2010. Antarctic subglacial conditions inferred from a hybrid ice sheet/ice stream model. *Earth and Planetary Science Letters*, **295**, 451–461.

PLANAVKSY, N. J., ROUXEL, O. J., BEKKER, A., LALONDE, S. V., KONHAUSER, K. O., REINHARD, C. T. & LYONS, T. W. 2010. The evolution of the marine phosphate reservoir. *Nature*, **467**, 1088–1090.

PYLE, L. J., NARBONNE, G. M., JAMES, N. P., DALRYMPLE, R. W. & KAUFMAN, A. J. 2004. Integrated Ediacaran chronostratigraphy, Wernecke Mountains, northwestern Canada. *Precambrian Research*, **132**, 1–27.

RAISWELL, R. & CANFIELD, D. E. 1998. Sources of iron for pyrite formation in marine sediments. *American Journal of Science*, **298**, 219–245.

RAMSAY, J. G. & HUBER, M. I. 1987. *The Techniques of Modern Structural Geology*, Vol. 2. Academic Press, New York.

ROSS, G. M. 1991. Tectonic setting of the Windermere Supergroup revisited. *Geology*, **19**, 1125–1128.

ROSS, G. M., VILLENEUVE, M. E. 1997. U–Pb geochronology of stranger stones in Neoproterozoic diamictites, Canadian Cordillera: implications for provenance and ages of deposition. *In*: Radiogenic Age and Isotopic Studies: Report 10. *Geological Survey of Canada Current Research*, **1997-F**, 141–155.

ROSS, G. M., MCMECHAN, M. E. & HEIN, F. J. 1989. Proterozoic history: the birth of the miogeocline. *In*: RICKETS, B. D. (ed.) *Western Canada Sedimentary Basin: A Case History*. Canadian Society of Petroleum Geologists, Calgary, 79–104.

RUELLE, J. C. L. 1982. Depositional environments and genesis of stratiform copper deposits of the Redstone Copper Belt, Mackenzie Mountains, N.W.T. *In*: HUTCHINSON, R. W., SPENCE, C. D. & FRANKLIN, J. M. (eds) *Precambrian Sulfide Deposits*. Geological Association of Canada Special Paper, **25**, 701–737.

SHEN, Y., ZHANG, T. & HOFFMAN, P. F. 2008. On the co-evolution of Ediacaran oceans and animals. *Proceedings of the National Academy of Sciences USA*, **105**, 7376–7381.

SHIELDS, G. A. 2005. Neoproterozoic cap carbonates: a critical appraisal of existing models and the plumeworld hypothesis. *Terra Nova*, **17**, 299–310.

SIEGERT, M. J., CARTER, S., TABACCO, I., POPOV, S. & BLANKENSHIP, D. 2005. A revised inventory of Antarctic sub-glacial lakes. *Antarctic Science*, **17**, 453–460.

SILVA-TAMAYO, J. C., NÄGLER, T. F. *ET AL*. 2010. Global Ca isotope variations in *c*. 0.7 Ga old post-glacial carbonate successions. *Terra Nova*, **22**, 188–194.

STEWART, J. H. 1972. Initial deposits in the Cordilleran Geosyncline: evidence of a Late Precambrian (<850 m.y.) continental separation. *Geological Society of America Bulletin*, **83**, 1345–1360.

TURNER, E. C. & LONG, D. G. F. 2008. Basin architecture and syndepositional fault activity during deposition of the Neoproterozoic Mackenzie Mountains supergroup, Northwestern Territories, Canada. *Canadian Journal of Earth Sciences*, **45**, 1159–1184.

TURNER, E. C., JAMES, N. P. & NARBONNE, G. M. 1997. Growth dynamics of Neoproterozoic calcimicrobial reefs, Mackenzie Mountains, northwest Canada. *Journal of Sedimentary Research*, **67**, 437–450.

UMER, M., KEBEDE, S. & OSMASTON, H. 2004. Quaternary glacial activity on the Ethiopian mountains. *In*: EHLERS, J. & GIBBARD, P. L. (eds) *Quaternary Glaciations – Extent and Chronology, Part III: South America, Asia, Africa, Australia, Antarctica*. Elsevier, Amsterdam, 171–174.

UPITIS, U. 1966. *The Rapitan Group, southwestern Mackenzie Mountains, Northwest Territories*. MSc thesis, McGill University, Montreal.

VOIGT, A. & MAROTZKE, J. 2009. The transition from the present-day climate to a modern Snowball Earth. *Climate Dynamics*, doi: 10.1007/s00382-009-0633-5.

WALLACE, M. W. & WOON, E. 2008. Giant Cryopgenian reefs as windows into pre-Ediacaran life. *In*: GALLAGHER, S. J. & WALLACE, M. W. (eds) *Selwyn Symposium 2008: Neoproterozoic Extreme Climates and the Origin of Early Metazoan Life*. Geological Society of Australia, Extended Abstracts, **91**, 17–22.

WARREN, S. G., BRANDT, R. E., GRENFELL, T. C. & MCKAY, C. P. 2002. Snowball Earth: ice thickness on the tropical ocean. *Journal of Geophysical Research*, **107**(C10), 3167, doi: 10.1029/2001JC001123.

WEIL, A. B., GEISMANN, J. W. & VAN DER VOO, R. 2004. Paleomagnetism of the Neoproterozoic Chuar Group, Grand Canyon Supergroup, Arizona: implications for Laurentia's Neoproterozoic APWP and Rodinia break-up. *Precambrian Research*, **129**, 71–92.

WEIL, A. B., GEISMANN, J. W. & ASHBY, J. M. 2006. A new paleomagnetic pole for the Uinta Mountain supergroup, Central Rocky Mountain States, USA. *Precambrian Research*, **147**, 234–259.

WINGHAM, D. J., SIEGERT, M. J., SHEPHERD, A. & MUIR, A. S. 2006. Rapid discharge connects Antarctic subglacial lakes. *Nature*, **440**, 1033–1036.

YEO, G. M. 1981. The Late Proterozoic Rapitan glaciation in the northern Cordillera. *In*: CAMPBELL, F. H. A. (ed.) *Proterozoic Basins of Canada*. Geological Survey of Canada Paper, **81–10**, 25–46.

YEO, G. M. 1984. *The Rapitan Group: relevance to the global association of Late Proterozoic glaciation and Fe-formation*. PhD thesis, University of Western Ontario, London (Ontario).

YEO, G. M. 1986. Fe-formation in the late Proterozoic Rapitan Group, Yukon and Northwest Territories. *In*: MORIN, J. A. (ed.) *Mineral Deposits of Northern Cordillera*. Canadian Institute of Mining and Metallurgy, Special Volume, **37**, 142–153.

YOUNG, G. M. 1976. Fe-formation and glaciogenic rocks of the Rapitan Group, Northwest Territories, Canada. *Precambrian Research*, **3**, 137–158.

YOUNG, G. M. 1982. The late Proterozoic Tindir Group, east-central Alaska: evolution of a continental margin. *Geological Society of America Bulletin*, **93**, 759–783.

YOUNG, G. M. 1988. Proterozoic plate tectonics, glaciation and Fe-formations. *Sedimentary Geology*, **58**, 127–144.

YOUNG, G. M. 2002. Stratigraphic and tectonic settings of Proterozoic glaciogenic rocks and banded Fe-formations: relevance to the snowball Earth debate. *Journal of African Earth Sciences*, **35**, 451–466.

ZIEGLER, P. 1959. Frühpaläozoische Tillite im östlichen Yukon-Territorium (Kanada). *Eclogae Geologicae Helvetiae*, **52**, 735–741.